Coordination Chemistry Reviews 255 (2011) 1480–1498

Contents lists available at ScienceDirect

Coordination Chemistry Reviews

journal homepage: www.elsevier.com/locate/ccr

Review

Creating and mastering nano-objects to design advanced catalytic materials☆

Gabriele Centi*, Siglinda Perathoner

Dipartimento di Chimica Industriale ed Ingegneria dei Materiali, CASPE/INSTM, University of Messina, Vle F. Stagno D'Alcontres 31, Salita Sperone, 98166 Messina, IT, Italy

Contents

ARTICLE INFO

Article history:
Received 18 August 2010
Accepted 8 January 2011
Available online 16 January 2011

Keywords:
Catalyst
Zeolite
Nano-reactor
Nano-confinement
Hierarchic structure

ABSTRACT

New developments in the synthesis of nano-materials have opened new possibilities for creating and mastering nano-objects in order to design novel advanced catalytic materials. This concise conceptual review will give a glimpse into this fast growing research area discussing some of the possibilities in this direction, the perspectives and the gap to reduce to develop selective catalysts for complex multi-step reactions. Emphasis is given to the opportunities offered by a tailored nano-design of the catalysts, from exploiting nano-confinement effects and supramolecular active sites synergies in nano-reactors to the new possibilities offered by new concepts such as the reduction of the relaxation time between two consecutive turnover cycles on a single active site and forcing a vectorial active site sequence in complex, multistep reactions. Other aspects discussed include the development of hierarchic pore structure to maximize catalyst effectiveness, metal complexes confined with solid cavities and the concept of nano-reactors, nanostructured composites and ordered 1D-type metal oxides. It is shown how significant progress in nano-materials has still not corresponded with progress in understanding the relationship between nanostructure and catalytic performance and the development of a more general strategy on the design of next-generation nano-catalysts.

1. Introduction

The significant changes in the worldwide economic and social panorama during the last decade have further stimulated the chemical and energy industries to reconsider their business strategies in terms of raw materials and energy resources, impact on the environment and the sustainability of their production [1–3]. One of the examples is the creation of the European Technology Platform on Sustainable Chemistry (www.suschem.org) from the joint effort of the European Chemical Industry Council (Cefic) and the European Association for Bioindustries (Europabio) to define a common vision and strategic roadmap to revitalize chemistry and biotechnology innovation in Europe. The aim was to strengthen the industrial competitiveness through a sustainability vision [4].

Because of these changes, a revitalization of the research on catalytic materials and industrial catalysts was observed in the last decade, with the opening of new area and in general a shift of the R&D activities with respect to those present in the last century [5]. For example, the increasing share of biofuels in the energy pool caused a fast growth in R&D activity to develop new catalysts and related catalytic processes [6,7]. Biomass is rich in oxygen and is composed of polymeric-like macro-units (cellulose, hemi-

☆ Realized in the frame of the activities of the EU Network of Excellence IDECAT (integrated design of catalytic nanomaterials for sustainable energy and production).

* Corresponding authors. Tel.: +39 090 6765609; fax: +39 090 391518.
E-mail addresses: centi@unime.it (G. Centi), perathon@unime.it (S. Perathoner).

0010-8545/$ – see front matter © 2011 Elsevier B.V. All rights reserved.
doi:10.1016/j.ccr.2011.01.021

cellulose, and lignin). Novel catalysts to deconstruct selectively these macro-units to smaller platform molecules (sugars, phenol derivatives, etc.) and to convert these by selective elimination of oxygen are necessary, while acid catalysis prevails in an oil refinery and catalysts able to insert oxygen into the hydrocarbon are necessary in petrochemistry. Thus, conceptually new catalysts are necessary to create a bio-based economy. In addition, several of the catalytic reactions for biomass transformation require combining homo/heterogeneous catalysis with biocatalysis, creating the need for new catalysts [7].

The push towards more sustainable industrial chemical processes has also accelerated the need for new catalysts to be able to perform in a single reactor more complex transformation to reduce process complexity, energy consumption and waste production [5]. Also in this case conceptually new catalyst design is required to achieve this goal [7]. The effort towards process intensification and the use of micro-reactors has also increased the need for a new catalyst design to improve the performance.

The last decade was also characterized by intense research effort on the synthesis of novel nano-materials [8,9], for example by (i) surface assembling [10] or nano-casting [11] to create tailored inorganic micro- and nanostructures, (ii) assembling nanoscale building blocks at solution/solid interface to create ordered tubular nanostructures [12], (iii) synthesizing novel nanostructured carbons (as tubes, fibers, graphenes, mesostructures, etc. with a variety of novel sp^2 and/or sp^3 configuration or functional properties) [13], (iv) using different assembling or template strategies to create 3D hollow nano-architectures [14] or multilevel interior-structured hollow 0D or 1D micro/nano-materials [15], (v) using aerogel or aerogel-like nanostructures to fabricate appropriate nano-scale building blocks with suitable void space and disorder as design components [16] or specific architecture (multiple junctions) in metal nanoparticles supported over metal oxides [17], where the presence of perimeter sites at the boundary between the metal nanoparticles and the oxide is important to determine the catalytic reactivity in simple reactions such as CO oxidation or water-gas shift reaction [18]. While increasingly sophisticated synthesis methods are available to control the (i) nanostructure of materials [19,20], (ii) hierarchic organization of the mesoscale in advanced materials [21–25], and (iii) nature of the active sites in nanoporous materials [26,27], still limited data are available, however, on the correlation between the nano-scale architecture of the catalysts and their catalytic activity, particularly in complex catalytic reactions [28,29] which are more demanding in terms of nano-architecture of the catalyst centres with respect to simpler reactions like CO oxidation or model reactions [30].

The existing gap with respect to the precise control possible in organometallic and metallo-organic catalysts has also been considerably reduced in solid nano-catalysts [31,32] in the last decade. This progress in R&D of tailored catalytic nano-materials put in a different perspective the traditional discussion about the advantages and limits of homogeneous versus heterogeneous catalysis [33–37] with the need to overcome this dichotomy in a new integrated vision [5]. This concise conceptual review has the aim to provide some of the potential possibilities, and reduce the aforementioned gap, in creating and mastering nano-objects for the design of advanced catalytic materials to address the societal challenging of sustainable production and energy [38].

2. Catalysis and the nano-dimension

Catalysis is a molecular phenomenon and similarly to homogeneous catalysis by metal-complexes in solid catalysis, the reaction occurs on an active site, i.e. involving the rupture and creation of bonds at the distance of the coordination sphere. However, a more rigid structure of the active centres is present and limited possibilities to tune the electronic structure of the active metal centre exist. Both these factors contribute to typically lower selectivities for heterogeneous catalysis in single reactions with respect to homogeneous catalysis by metal complexes, although the former are able to perform selectively complex multistep reactions, which often cannot be made by homogeneous catalysts [5].

The surface sites on a solid material (for example, hydroxyl groups) may act as ligands to prepare supported metal complexes, in order to combine the advantages of homogeneous catalysts (better intrinsic control of the nature of the active centre) to those of heterogeneous catalysts (easy separation, higher productivity, etc.), and also to prepare single site catalysts. This was the base concept for the large effort towards a “surface organometallic chemistry” [39]. However, the surface sites present on the support may interact with the metal complexes. This interaction often gives rise to a lowering of the performance of the supported metal complex with respect to those of the analogous homogeneous complex. An approach explored to overcome this problem was to tether covalently the metal complex to the supports, i.e. to introduce a flexible spacer (linker) between the metal complex and the support [40–43]. In some cases, the supported metal-complexes showed improved performance [44,45]. The direct anchoring of the metal complex to the surface through covalent bonding may change the electronic state of the metal centre or force an unusual configuration of the metal complexes, which can reflect positively in its reactivity or can improve the performance by assisting the coordination of the incoming molecules. Novel active reaction spaces can be thus designed by (i) influencing the coordination of the central metals, (ii) chemical interaction at metal–surface interface, and (iii) three-dimensional architecture at the surface sites [37,46]. Therefore, not only the specific nature of the active centre, but also the environment around the active sites is relevant in determining the catalytic behaviour, similarly to enzymes where the flexible protein-structure determines the access and coordination of the reactants to the active sites.

Additional effects are possible due to the presence of an ordered 3D structure. A good example is offered from microporous (zeolite) materials having active site centres located inside the ordered pore structure. Due to the molecular-size dimensions of the channels and access cavities in microporous materials, the well-known effects of shape selectivity are present: restriction on diffusion of reactants and/or products, and on transition state [47–49]. Chiral zeolitic materials can also combine both shape selectivity and enantioselectivity [50]. Another effect is related to the change in the local nano-environment. This concept can be exemplified by the case of Ti-silicalite (TS-1), industrial catalyst for the selective oxidation of various substrates using H_2O_2 [51]. TS-1 has approximately the same composition as the Shell epoxidation (industrial) catalyst based on Ti ions supported on amorphous silica [6]. Both these catalysts are selective in the synthesis of propene oxide from propene, but TS-1 uses H_2O_2 as the reactant, while hydroperoxides (for example, ethylbenzene hydroperoxide) are necessary in the case of the Shell catalyst [5]. The difference is related mainly to the local environment around the Ti active sites. TS-1 is hydrophobic and water molecules essentially do not diffuse inside the channels of TS-1 zeolite, where the Ti ions are localized. In the Shell catalyst the Ti ions are accessible to water molecules. The catalyst is able to epoxidize 1-hexene with H_2O_2, if a “water-sponge” is present which scavenges the H_2O formed during the reaction. TS-1 is instead active in aqueous solutions of H_2O_2 (usually a water/methanol solvent is used), because the hydrophobic character of the local environment around the active sites (nano-environment) creates a local water-free-like solvent.

The differences in the hydrophobic character between silicalite (TS-1) and silica (Shell catalyst) derives from the presence of a well ordered structure which creates an ordered array of channels (therefore, minimizing defects) in the first case, while defects in amorphous or crystalline silica create hydroxyl groups (silanols) or hydroxyl nests which induces some degree of hydrophilic character in the Shell catalyst. These hydroxyl groups under acid catalysed conditions (acidity is generated by oxidation of the solvent) cause ring opening to the corresponding glycol in the soon to be formed epoxide. In addition, the water adsorbed on the surface limits the accessibility of the alkene towards the active centre. Partially hydrophobic materials can been obtained by anchoring TiF_4 on silica [52] or by anchoring alkyl (alkoxy) groups to the silica surface [53]. The amorphous microporous titania–silica in which pendant alkyl groups make the surface hydrophobic is able to epoxidize alkenes with H_2O_2 [54].

This example illustrates the concept that the confinement of active centres or catalytic nanoparticles inside a micro- or mesoporous ordered material may significantly change the reactivity properties [55–59].

Rolison in her paper in Science [16b], extending the original work on Au–TiO_2 composite aerogels for CO oxidation [17] to Pt-colloid-modified carbon-silica composite aerogels argued the unimportance of periodicity. Rolison et al. [16a] have further extended the concept in a more recent review to the design of the nano-architecture of materials for various energy storage and conversion applications, such as electrodes for PEM fuel cells, supercapacitors, ion-batteries, etc. They showed, for example, that aerogel-based nano-architectures (quasi-3D mesoporous architectures made up of covalently bonded nanoparticles that form essentially 1D networks) do not exhibit grain-boundary impediments to transport, e.g. protons on manganese oxide [16c] or oxide ions at 600 °C in Gd-doped ceria [16d]. However, these effects are relevant when surface ion-transport is important, such as in electrodes, but not in heterogeneous catalysts, where this transport mechanism is not relevant.

Nevertheless, the question is whether an ordered nanostructure or periodicity is necessary, although the presence of a large number of industrial catalytic processes, in the refinery, petrochemistry and fine chemicals sectors based on zeolites [48] already pointed out the relevance of materials having an ordered porosity.

As remarked by Antonietti and Ozin [25], periodicity in materials gives a maximal structural density with minimal surface area, while aerogels having a fractal order can maximize the surface area, even though under most of the industrial relevant catalytic reactions they do not show enough stability or mechanical resistance. However, apart from the issue of stability, the conceptual question is whether an intrinsic order (nano-architecture) in the material is necessary. In relatively simple reactions such as CO oxidation, where the maximization of the number of the active sites at the interfacial region between the gold nanoparticles and the support could be the important aspect [17], a fractal-type material such as aerogels could be more active. However, in general this type of materials is intrinsically more heterogeneous in terms of active sites and shows the presence of many defects. In more complex and industrially relevant catalytic reactions, the critical aspect is the selectivity rather than the activity [51]. It is required ideally to have a unique type of active site, and an increase in the surface area favours the presence of an heterogeneity of active sites negative for the selectivity. For example, most of the industrially used mixed oxides in selective oxidation reactions have a low rather than a high surface area [51]. For this reason, a periodic nanostructure is preferable, because this can combine a high surface area to a regular local nanostructure. In addition, it offers additional advantages as discussed above, for example in terms of confinement or shape selectivity.

For a more complete understanding of shape selectivity, it is necessary to understand the effect of confinement on the various kinetic and thermodynamic factors that can influence the outcome of a zeolite-catalysed reaction [49].

In microporous materials, where the channels have molecular dimension, Derouane [60] originally proposed the idea that the zeolite itself could be considered as a solid solvent and thus the behaviour of molecules inside the zeolites results from solvation effects. Gaussian curvature of zeolitic structures and dispersion self-energy of molecules (analogous to the Born electrostatic self-energy of an ion) have to be accounted for the adsorption properties of zeolites [61]. A molecule inside a zeolite channel behaves differently from outside, and not only for steric restrictions on diffusion or transition state.

In a similar approach to these phenomena, Corma and coworkers [59] suggested that molecules in zeolites are confined at the molecular level, i.e. the molecular orbitals are strongly perturbed by the solid. They showed that the aromaticity of anthracene in zeolites was strongly disrupted due to limitation of the π-orbital spatial extension induced by the pore walls proximity. This indicates that the localized approach of active sites inside a microporous material is not truly correct, i.e. the reactivity of a metal centre located in the zeolitic cages (for example, Cu ions inside a ZSM-5 zeolite) is influenced from the surrounding cage, even beyond the steric (shape selectivity) constrains. Thomas [62], for example, studying the effect of co-adsorbed solvent molecules on the photoinduced processes in zeolite cavities demonstrated the unique charge trapping and charge stabilization effect of the zeolite confinement.

These results further indicate the concept that the nano-environment around the active sites (confinement) influences the reactivity beyond the possible effects related to steric constrains or diffusional limitations.

2.1. Nano-confinement

Confinement effects were also observed in mesoscale ordered materials such as MCM-41 and SBA-15, where the steric restrictions on the diffusion and/or transition state (e.g. shape selectivity) are not present due to the higher diameter of the channels (>1 nm). We define here nano-confinement, the presence of confinement effects in restricted spaces with few manometers scale. Fajula and coworkers [63] showed that curvature strongly altered the liquefaction free energy of hexane in MCM type materials. By NMR it was shown that molecular motion was strongly anisotropic close to the pore walls of silica [64]. Cros et al. [65] showed that the chemical shift of ^{129}Xe adsorbed on mesoporous silica was pore size dependent. By large angle X-ray scattering it was shown that methanol confined in MCM-41 was highly ordered within the pores and the density of confined methanol was higher than that of bulk methanol, varying regularly along the diameter of the pore [66,67].

There are thus various demonstrations that surface effects tend to become dominant in fluids confined at the mesoscale and that the molecular properties may become anisotropic close to the channel walls, depending on the Gaussian curvature of the latter. In fact, above around 5 nm these confinement effects are usually no longer observed.

These confinement aspects influence the catalytic behaviour, although data are limited. A predictive model of confinement effects at the mesoscale is also missing. The microscopic pressure within a confined liquid could determine a pseudo-enhancement of the local pressure. Baiker et al. [68] studying near-critical CO_2 in mesoporous silica by in situ FTIR demonstrated that the CO_2 density was always higher in the silica pores than in the bulk, even under supercritical condition. Other effects of confinement are the lowering of entropic barriers and the wetting of nanorough surfaces.

Gounder and Iglesia [69] showed that in n-alkanes conversion the acid sites confined within 8-MR pockets of the zeolite are much more active for monomolecular isobutane reactions than sites of similar acid strength within 12-MR channels, because partially confined transition states have lower standard free energies as a result of entropy–enthalpy trade-offs. Partial dewetting in confined structures could result in strong pressure increases within the confined liquid [70].

There are thus different possible effects and interpretations of the confinement effect. The common feature is that in mesoporous materials having channel size ranging between 1 and 5 nm the properties of reactants/substrates can be influenced by the nanometric confinement and/or the presence of a curved surface (inside the channels of the mesoporous ordered materials) with respect to on an ideally flat surface, and this in turn reflect in different reactivities. The presence of an ordered mesostructure formed by regular channels (in MCM-41 and SBA-15 materials) determines the presence of these effects, which are not present for an irregular assembly of nanoparticles such as in aerogels.

There is increasing research interest in how this mesoscale nano-confinement influences the properties beyond catalysis. For example, de Jongh and Adelhelm [71] have reviewed the recent research on the concept of nano-confinement as a new strategy towards meeting hydrogen storage goals. Huck [72a] and Wu et al. [72b] have discussed how, in a physically confined environment, interfacial interactions, symmetry breaking, structural frustration and confinement-induced entropy loss determine a molecular organization of materials located inside ordered mesostructure such as SBA-15 which determine a change of their physicochemical properties.

The nano-confinement also influences the properties of metal nanoparticles. Bao and coworkers [73–76] have extensively investigated this concept, particularly in relation to how it is possible to modify the redox properties of transition metals via confinement within the channels of carbon nanotubes (CNTs), in order to change their catalytic performance.

For example, the reduction of Fe_2O_3 nanoparticles is significantly facilitated inside CNTs compared to those on the outside [74]. In situ HRTEM indicated that the CNT-confined Fe_2O_3 particles transformed to metallic iron at 600 °C, while the outside particles remained oxidized at this temperature. They also showed [75] that confinement within carbon nanotubes modifies the reactivity of iron catalysts in Fischer-Tropsch (FT) synthesis. The iron species encapsulated inside CNT are stabilized in a more reduced state and the formation of iron carbides under the reaction conditions is enhanced. The latter have been recognized to be essential to obtain high FT activity. The relative ratio of the integral XRD peaks of iron carbide (Fe_xC_y) to oxide (FeO) is about 4.7 for the encapsulated iron catalyst in comparison to 2.4 for the iron catalyst dispersed on the outer walls of CNTs. This causes a remarkable modification of the catalytic performance. The yield of C_{5+} hydrocarbons over the encapsulated iron catalyst is twice that over iron catalysts outside CNT and more than 6 times that over activated-carbon-supported iron catalysts. Also in the electrochemical reduction of CO_2 to isopropanol and other alcohols/hydrocarbons, the iron-particles located inside the CNT show enhanced properties with respect to those located on the outer surface [77].

In the syngas conversion to C2 oxygenates such as ethanol, acetic acid and acetaldehyde, Rh–Mn particles located inside the CNT show a higher activity than when located on the outer surface [73c]. RhMn in the CNT interior likely exists in a more reduced state than that on the exterior and this fact modifies the mechanism of CO adsorption, as demonstrated by Raman spectroscopy [73c]. In addition, theoretical studies combining first-principles and Monte Carlo simulations indicate the stronger interactions of both H_2 and CO with the interior nanotube surface than with the exterior surface, but the effect is different for the two molecules. As a result, not only a pseudo-enhanced pressure within the CNT is present, but also the CO/H_2 ratio is altered. The effects are depending on the diameter of CNT. The enrichment generally becomes more significant inside smaller nanotubes at lower temperatures and higher pressures.

There is thus growing evidence that both the adsorption and reactivity of the reactants and the nature of the active sites (metal nanoparticles) are influenced by the nano-environment and -confinement inside ordered nano/meso structures and in turn, these aspects influence the catalytic behaviour beyond possible effects of shape selectivity. Locating metal nanoparticles inside CNT [78] and more generally in a confined nano-environment is thus an opportunity to control and enhance the catalytic performance. Note that this concept is different from that of interface sites between active particles and the support [79,80], where new type of active sites generate due to the interface. Bao and coworkers [81] observed recently that two-dimensional FeO nanoislands may be formed on Pt(1 1 1) surface and that coordinatively unsaturated ferrous (CUF) sites form at the interface. These CUF sites show high activity in the selective oxidation of CO. They attributed the stability to an interface confinement [81], but the effect may be more properly described as deriving from a metal-support strong interaction and the generation of new sites at the interface. The nano-confinement is instead related to a local change of the characteristics of the reaction medium due to confinement, while the nano-environment indicates the presence of co-catalytic effects in the supramolecular environment around the active site.

3. Self-assembly of nano-reactor

An extension of the concepts discussed in the previous section is that of nano-reactors. One possibility is to use organized assemblies, including supramolecular aggregates, colloidal structures (e.g., micelles, microemulsions), liquid crystals, dendrimers, and mono- and multi-layers. The effects on the reactivity may be classified in four areas [82]:

(i) the enforced juxtaposition of functional groups in the organized assemblies that leads to intramolecular reactivity or cooperative catalysis (proximity effect, similar to neighbouring group participation in small molecules);
(ii) diffusion of reagents into the interior of the organized assembly that leads to a microenvironment different from the bulk solvent (solvent effect);
(iii) unique properties of the interface between the organized assembly and the bulk solvent (interface effect);
(iv) the confinement of molecules within the restricted space of the organized assembly (steric effect).

In organized assemblies, co-catalysis by neighbouring group participation can lead to dramatic rate acceleration and unexpected changes in the selectivity. The difference with respect to a metal-complex is that these co-catalytic functional groups are brought together by spontaneous assembly rather than through synthesis. The effect is often observed in organo-catalysis [83]. Apart from facilitating reactions between neighbouring groups, organized assemblies can catalyse chemical reactions by making adjacent catalytic centres acting cooperatively.

In heterogeneous catalysis, a similar concept is used to develop multifunctional catalysts for fine chemical synthesis, using for example the properties of layered compounds to spatially separate catalytic functions which otherwise interfere each other [84]. An interesting example is when a reaction requires in cascade both strong acid and base Brönsted sites, because they tend

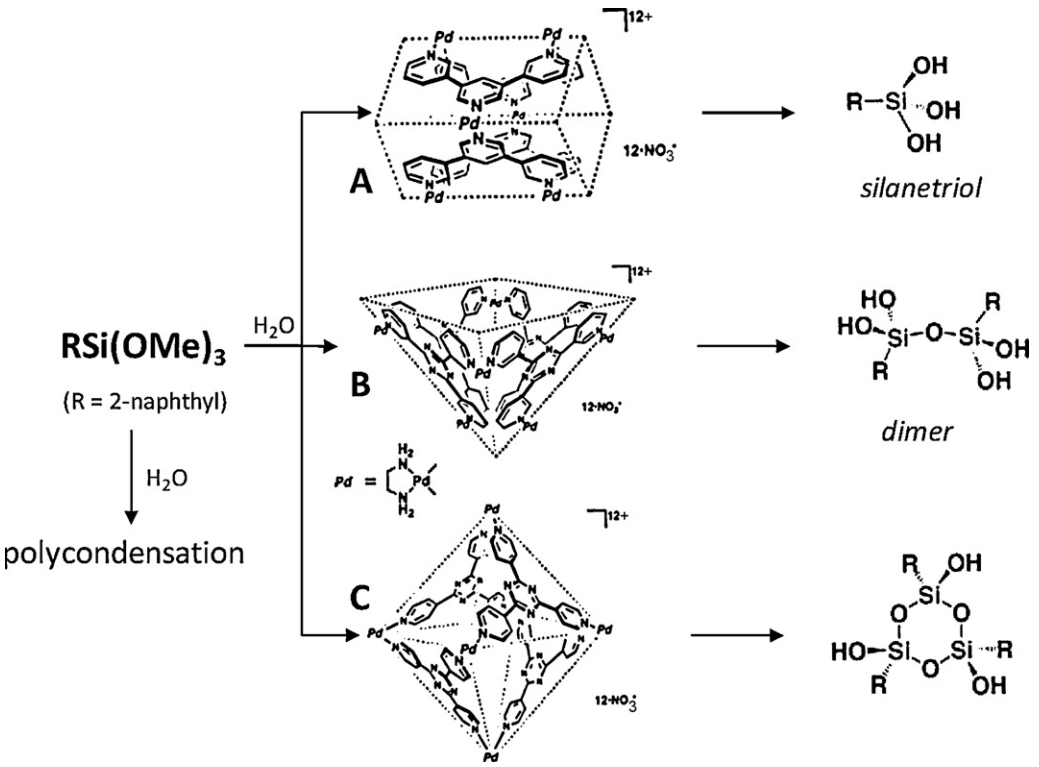

Fig. 1. Cavity-directed synthesis in the selective oligomerization of trialkoxysilanes. Adapted from Ref. [90a].

to self-neutralize. Kaneda and coworkers [85] used an interesting approach to solve the problem. They localized strong acid sites inside the layers of montmorillonite clay by inserting Ti^{4+} ions, and used as base Brönsted sites those present on the external surface of the hydrotalcite particles. Because the Ti(IV)-montmorillonite has active acid sites in the narrow interlayers, the base sites of large HT particles show no interaction with the acid sites. In the one-pot synthesis of benzylidene malononitrile from malononitrile with benzaldehyde dimethylacetal (an example of tandem deprotection–aldohol reaction with acids and base different steps) an overall yield of 93% was observed using Ti^{4+}-montomorillonite and hydrotalcite in close interaction. The approach may be extended to a variety of acid and base reactions, such as esterification, acetalization, deacetalization, aldol reaction, Michael reaction, and epoxidation [84,85].

In organized assemblies, the reagents and products can diffuse in and out depending on the polarity of the microenvironment, and thus the phenomena of reagent/products accumulation or change in the solvent characteristics may occur inside micelles or micro-emulsions with a consequent influence on the reactivity [86]. There are many examples of how the reactivity changes in these nano-reactors and about the versatility of the heterogeneous environment in micro-emulsions to influence the reactivity and catalytic performance. The reactivity of oxovanadate species depends on their degree of condensation. In isooctane reverse micelles (RM), vanadate dimerization (and formation of more condensed species such as tetrameric and pentameric oxovanadate) at neutral and basic pH is higher compared to bulk aqueous solutions, due to the establishment of a proton gradient from the RM interior towards the periphery [87]. The solvent dynamics inside RM are also different with respect to those in the bulk solvent. Fayer et al. [88] observed that the nanoscopic confinement inside RM has a major impact on the water hydrogen bond network dynamics regardless of the nature of the interface. In other words, the nano-confinement itself influences the properties of the solvent molecules in the container. Finally, the limited space and restricted mobility within the organized assemblies can also affect the mechanism/rate of reactions, similarly to what discussed in zeolites.

Chen et al. [89a] reported recently that Pd nanoparticles in mesoporous silica hollow spheres show significantly superior activity in Suzuki coupling reactions with 99.5% yield in few minutes of reaction. Mahmoud et al. [89b] demonstrated that the frequency factor in Arrhenius plot studying the catalytic reduction of 4-nitrophenol is significantly enhanced due to nano-reactor confinement in hollow nanoparticles. There are thus growing results showing the possibility of preparing enhanced catalysts using the nano-reactor concept.

3.1. Self-assembled cages and nano-containers

In recent years, many studies were published on the preparation of self-assembled cages as artificial cavities to trap and isolate molecular guests. Compared to covalent cages, self-assembled containers are simpler and more economical to prepare, because essentially it is necessary only to mix the molecular components, forming the cage with the guest in solution; the reacting host–guest complex is generated spontaneously.

Fuijta and co-workers [90] have significantly contributed to efficiently synthesize a large variety of nanoscale molecular cages (also called “nanovessels” or “nanoreactors”) by following a transition metal-mediated self-assembly methodology using six metal centres (e.g., Pd(II) and four tridentate ligands. Fig. 1 illustrates the concept of how the presence of a nanoscale molecular cage (self-assembled hollow compounds) determines the selectivity in the simple reaction of hydrolysis of trialkoxysilanes [90a]. Pd(II)-linked coordination hosts (tube, bowl or, cage; A, B and C in Fig. 1, respectively) strictly control the oligomerization of trialkoxysilanes, $RSi(OMe)_3$ (R = 2-naphthyl). Within nanocage A, one molecule of trialkoxysilane is accommodated and subsequently hydrolyzed to give silanetriol $RSi(OH)_3$. Under ordinary aqueous

conditions, this reactive compound undergoes rapid polycondensation (sol–gel condensation) leading to Si–O networks. Within the cavity of nanocage A, however, the polycondensation is suppressed. Nanocage B and C give its dimers $RSi(OH)_2OSi(OH)_2R$ and cyclic trimers $[RSi(OH)O]_3$, respectively.

The nanocage C (Fig. 1) also enhances the rate of photodimerization of olefins and especially to give perfect regio- and stereoselection, and high pairwise selection (when two different olefins are used) giving only the cross [2 + 2] adduct [90b,c]. The dimerization of acenaphthylenes and naphthoquinones quantitatively proceeded in the cavity with remarkable rate acceleration and perfect regio- and stereo-control (>98%) [90b].

A wide array of self-assembled molecular nanocages based on various building blocks and noncovalent interactions has been developed in the last decade [91]. The nanospace within these supramolecular capsules is generally in the range of 30–50 nm, which is sufficient for the selective encapsulation of one large or a number of smaller molecules. The size is comparable to that of silica mesoporous materials such as MCM-41 or SBA-15. With respect to other assemblies such as vesicles and micelles [92], we could comment that in the latter a distribution of sizes (more or less narrow) instead of a specific size is present. Micelles are thus less-defined systems when compared to vesicles or self-assembled capsules with respect to both shape and kinetic stability. In addition, the shape and size of a micelle is a function of the solution conditions such as surfactant concentration, temperature, pH, and ionic strength, besides that of the molecular geometry of the surfactant molecules. They have the advantage of lower cost, but allow a less precise control of the nano-environment.

Organic reactions in water aided by surfactants to form micelles have been known for a long times, but only more recently have micelles been explored as catalytic nano-reactors for industrial relevant reactions. An example is the enantioselective Baeyer–Villiger oxidation of cyclic ketones using environmentally friendly oxidants [93]. The reaction was carried out in water by using soft Lewis acid Pt(II) complexes that have chiral diphosphines as well as monophosphines. Addition of a surfactant is crucial, which leads to the formation of micelles that act as nano-reactors. For the oxidation of meso-cyclobutanones, addition of surfactants allowed the reaction to proceed in high yields and the enantiomeric excess (*ee* of 56%) was higher than in organic solvents. For meso-cyclohexanones the yields are lower, but enantio-selectivity is higher (*ee* up to 92%) moving from organic to water–surfactant media. Micellar systems were also used for the enantioselective catalytic hydrogenation (with Rh complexes) not only to improve the performance, but also to facilitate catalyst recovery and recycling [94].

Microemulsions could be also used to prepare and stabilize metal nanoparticles in water [95a] and realize ligandless metal catalysts. For example, colloidal palladium stabilized by surfactants in water could be successfully used in a number of catalytic reactions: the Suzuki–Miyaura reaction, arylation of olefins (the Heck reaction) and carbonylation of aryl iodides [95b]. The yield of the reaction correlates with the stability of the Pd sol, but the separation of the colloidal catalyst is difficult.

The alternative is to use palladium nanoparticles stabilized by water-soluble diblock copolymeric micelles [95b]. Diblock copolymers consisting of lyophilic and lyophobic blocks, upon dissolution in a selective solvent (dissolving only one block), self-organize in micelles in which the lyophobic block forms a dense core, and lyophilic block forms a diffuse micelle corona. In water the hydrophobic block forms a core, and the hydrophilic one, a corona of a micelle. On the other hand, in a nonpolar solvent the core contains the hydrophilic block. Therefore the immobilized metal nanoparticles, due to interaction with the hydrophilic block, are located in the core of the micelle. In the latter, the reduced accessibility of the metal nanoparticle in the core reduces the catalyst activity.

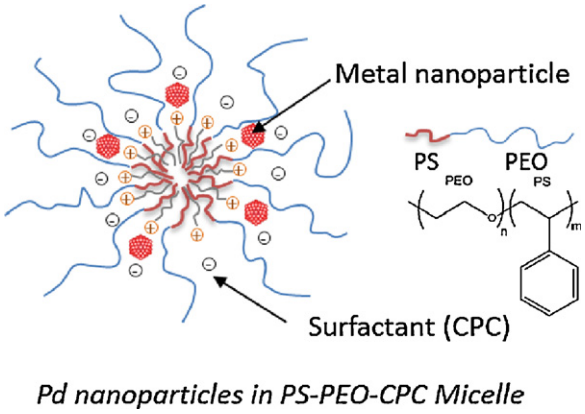

Fig. 2. Palladium nanoparticles stabilized by water-soluble diblock copolymeric micelles.
Adapted from Ref. [95b].

A better solution is not to locate the metal nanoparticles in the core or in the corona, but rather in their interface. An example is given from the amphiphilic diblock copolymer of polystyrene–poly(ethylene oxide) (PS–PEO) dissolved in water with addition of surfactant (cetylpyridinium chloride – CPC). The hydrocarbon chains of the latter penetrate the hydrophobic core of a micelle formed by the polymer, with the charged groups left on the interface, giving to it a positive charge. Addition of K_2PdCl_4 leads to adsorption of anions of $PdCl_4^{2-}$ on the interface of the core of a micelle [95b]. The palladium (II) is reduced by KBH_4, forming nanoparticles adsorbed on the interface of the core of a micelle (Fig. 2) [95b]. A main limitation is the stability of the assembly, which cannot be used at temperatures above 60 °C. However, the catalyst shows rather interesting performance in the olefin arylation reaction (the Heck reaction), carbon–carbon bond formation (Suzuki–Miyaura reaction) and other reactions [95b].

There are various alternative ways to stabilize metal nanoparticles in solution, for example using dendrimers [96,97] which offer the advantages of a precision of the dendrimer structures and a specific topology coupled to a variety of dendrimer generations. Seminal studies by van Leeuwen and Brunner's dendrizyme concept [98a,b] opened the field of dendrimer catalysis. With peripheral catalyst loading, the multiple sites provide an exceptional density of catalysts, but steric constraints limit the access to the catalytic centres. Star-shaped catalysts or first generation "dendrimers" coupled catalysts are as efficient as mononuclear catalysts with easy recovery and re-use, contrary to mononuclear catalysts. In the Pd-catalysed Suzuki–Miyaura reaction turnovers up to 10^6 were obtained [96].

There are many other possible approaches to produce self-assembled nano-reactors [92]: vesicle-based systems, macromolecular and biomacromolecular nanoreactors. At the end of last century, lipid-based vesicular assemblies as potential cell membrane mimics and subsequently as enzyme and catalyst-containing nano-reactors received considerable attention, but successes were limited. The development in supramolecular chemistry made available, however, a wide variety of building blocks which opened new possibilities to create nano-cages by self-assembly. In areas such as drug delivery, this R&D effort has led to a number of commercial applications, but in the field of industrial catalysis commercial applications are instead still limited. Recent advances includes the formation of vesicle systems (polymersomes) with ionic liquid interiors dispersed in water [99] which offer interesting opportunities both as nano-carriers or as nano-reactors for catalytic reactions.

These examples of self-assembled cages and nano-containers require operating in solution and in mild reaction conditions, i.e. they can be used for catalytic reactions of possible interest for fine chemical production or organic syntheses. From an industrial perspective, this class of reactions has limited production volumes and usually it is necessary a fast development of the synthesis procedure on an industrial scale (often on a few month time scale). Both these aspects greatly limit the possibility to introduce new catalytic routes.

For the production of larger volume chemicals, continuous operations, low cost of separation and especially productivity are the key elements for the success of a new process [5]. While often attention is put on the turnover and related aspects (i.e. specific activity per site), productivity per reactor volume is industrially more relevant. The nano-reactor approaches discussed above have an intrinsic limit of the need to operate in mild conditions and often under diluted concentrations, both aspects negative to obtain high productivities. In addition, dispersed systems in a solvent require high cost for reactor efficient mixing, and high separation costs, even though the use of surfactants may facilitate the separation. The presence of leaching and the long-term re-usability of the catalyst are further potential issues. Notwithstanding the significant progresses and stimulating results obtained in the last one-two decade in the field of self-assembled nano-reactors, their industrial application is still quite limited for the motivations discussed above. The question is thus whether the concepts of self-assembly of building blocks (nano-objects) to prepare nano-reactors could be translated to inorganic (solid) catalysts operating in a heterogeneous phase, to develop next-generation industrial catalysts.

4. Building catalyst nano-architecture

Industrial solid catalysts are typically used in pellets of size some mm. Therefore, the design of the catalyst should consider also the micro-scale optimization of the pore structure together with the molecular and nanoscale aspects discussed in the previous sections, in order to guarantee (i) an easy access of the reactants (important to avoid mass transfer limitations which influence the reaction rate) and (ii) a fast desorption of the products (which influence the secondary reactions and thus the selectivity, besides to be potentially also a rate limiting step) [100].

Significant R&D attention has been given recently on developing hierarchic-organized catalysts [101–105], particularly in the field of zeolites, to develop materials with optimized pore structure to allow an improved accessibility and molecular transport.

Zeolites and in general materials with active sites confined in micropores show often severe mass-transfer limitations, particularly for large crystals and when uni-dimensional pore structure is present. In fact, there is a conflict in diffusion between reactant coming in and products going out of pores having molecular dimensions. When instead a 3D pore channel is present in the zeolite, a kind of molecular traffic control exists where reactants and products diffuse along different paths [106–108], reducing but not eliminating diffusional limitations. In a typical zeolite crystal with size in the micron range, the diffusional path of the molecules to have access to the active sites located in the inner part of the crystal is quite long (a factor about 10^2–10^3 in the ratio between pore and molecule lengths). In addition, technical catalysts have dimensions of the pellets ranging from 50 to 100 μm for catalyst transport and fluid-bed reactor applications to mm range for mobile and fixed bed reactor applications.

Diffusion limitations due to restricted access and slow transport to/from the active site determine low catalyst utilization, which is described from an engineering point of view in terms of effectiveness factor. This fact represents a major drawback in most industrial reactions catalysed by zeolites, e.g. cracking, oxidation, (hydro)isomerisation, alkylation, and esterification, as they do not operate at their full potential.

The diffusion regime in mesopore catalysts is typically bulk or Knudsen diffusion and this leads to diffusivities several orders of magnitude higher than in micropores. Therefore, one common way to reduce diffusional limitations is to use suitable binders (typically based on silico-alumina) which have mesoporosity and connect the various zeolite crystals to form the pellet with the necessary technical size for application. The binder has also additional functions, from giving the necessary mechanical strength to act sometimes as co-catalysts. The further steps are to optimize the pore engineering of the zeolite crystals and/or to reduce the dimensions of the zeolite crystals.

4.1. Assembling zeolitic nano-units

Protozeolitic nano-clusters (or units) indicate the early stage of synthesis of zeolite, where already the unit elements of the zeolite structure are present, but the dimensions of the particles are very small, few tens of nanometers. These materials show potentially the same characteristics of zeolites, but have virtually no problems of diffusivity due to the very small dimensions. However, there are some main drawbacks: (i) the recovery from the crystallization gel is difficult, (ii) the units tend to aggregate and (iii) the surface to bulk ratio is quite high. The sites present on the surface of the nano-crystal have different properties with respect to the analogous located inside the zeolite channels, for the motivations discussed before. An approach recently developed for preparing hierarchic-organized catalysts from protozeolitic units is based on their surface-passivation by silanization [109]. Organosilanes (for example, 3-aminopropyltrimethoxysilane, isobutyltriethoxysilane, phenylaminopropyltrimethoxysilane and octadecyltrimethoxysilane) are grafted onto the external surface of the zeolitic nanounits hindering their further aggregation, inhibiting their surface reactivity, and allowing to develop materials with hierarchical porosity and enhanced textural properties. Fig. 3 schematically illustrates this type of mesopore assembling of protozeolite units grafted with organosilanes (phenylaminopropyltrimethoxysilane, PHAPTMS) [109d]. It is also given an example of the catalytic performance of these materials in the anisole Friedel Crafts acylation. It is shown that catalysts prepared from ZSM-5 protozeolite allow an improved conversion of anisole with respect to commercial ZSM-5 samples, with an improvement of the catalytic performance on increasing the amount of organosilane (PHAPTMS) used during the preparation [109d].

Surface-passivating silanization of protozeolitic units is an effective strategy for the preparation of zeolite nanocrystals with a controlled aggregation degree, a hierarchical porosity and relatively uniform mesoporosities [109a]. The mean sizes of the nanounits and, therefore, the textural and accessibility of these materials can be varied by changing the precrystallization conditions and the concentration of the seed-silanization agent. The resulting combination of mesopore sizes and exterior-nanocrystal surface properties of the hierarchically structured zeolites allow to develop catalysts active in reactions that are otherwise strongly limited by steric and/or diffusional limitations, for example in the polyethylene cracking [109a].

The creation by silanization of a secondary porous structure connecting the zeolite crystals has a further relevant role on the reactivity, as shown recently by Lercher et al. [110]. Sorption into the zeolite channels proceeds via a weakly bound physisorbed and nonlocalized state on the external surface as the dominating reaction pathway. The weak interaction leads to very low sticking probabilities of the order of 10^{-7} [110b]. When a mesoporous silica overlayer is created over the zeolite crystals to prepare

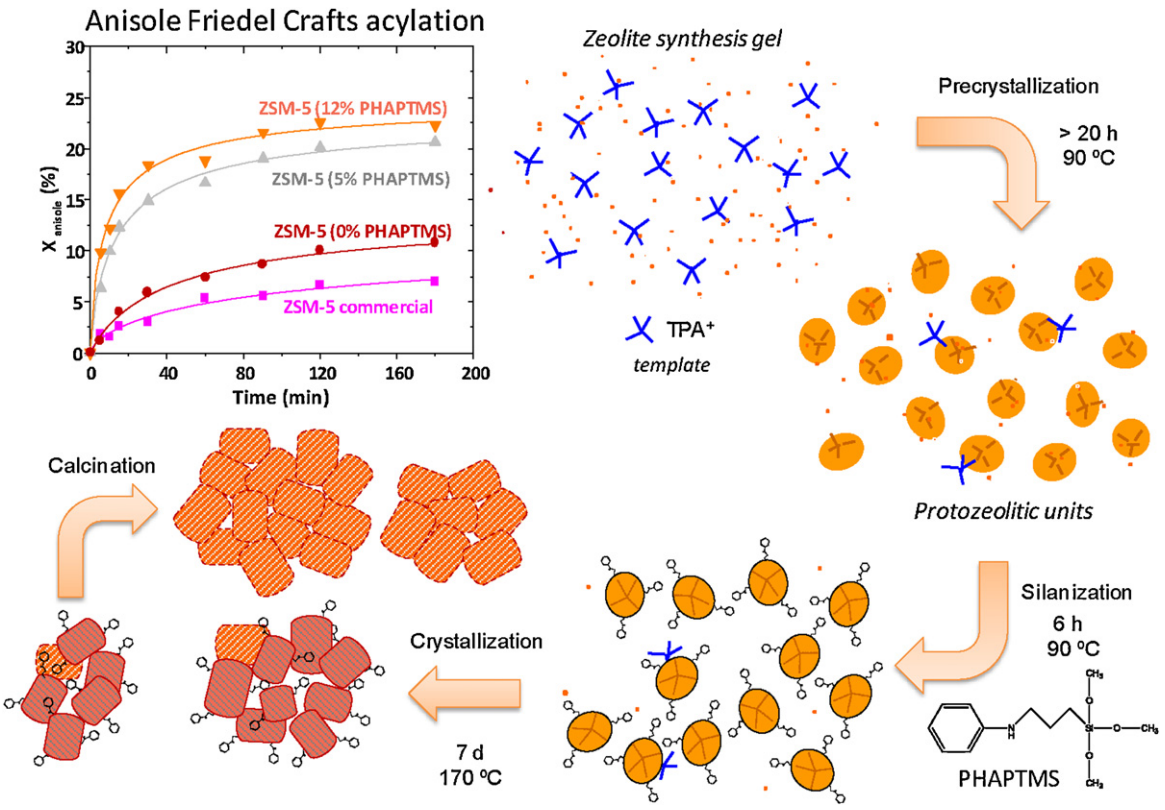

Fig. 3. Mesopore assembly of protozeolite units grafted with organosilanes and their behaviour in the catalytic anisole acylation. Adapted from Ref. [109].

hierarchical-organized materials, there is a significant increase in the sorption rates.

For the unmodified zeolite, molecules originated from the gas phase collide (a) with the zeolites surface and a physisorbed state is populated followed by pore entering and intracrystalline diffusion. On modified zeolites, they primarily impinge with the silica surface overlayer, and with a certain probability, they can directly enter the overlayer porosity. A subsequent step is necessary here to access the crystalline zeolite core hidden below this overlayer. Those molecules, having trajectories distinctly tilted from the perpendicular plane of the pore opening, are instantaneously rejected to the gas phase. Consequently, the overall transport process to the sorption sites inside the pores can be divided into two coupled regimes. The first is the transport of sorbate molecules through the interface between the gas phase and the amorphous overlayer, and the second is the transport from the amorphous overlayer into the micropore openings. The total mass flux of the sorbate molecules to the sites inside the pores is thus influenced by the ratio between the overlayer pore dimensions and the gyration radius of the sorbate (controlling the probability of the molecules for entering into the overlayer pores) and the ratio between the diameter of the zeolite micropores and the kinetic diameter of the sorbate.

Consequently, chemically modifying the outer zeolite surfaces introduces novel strategies to improve current industrially relevant separation and catalytic processes. In contrast to the well-known concept of pore aperture adjustment to enforce shape selectivity by overall retardation of transport processes, well-defined hierarchical overlayer architectures and porosities could be utilized as a powerful method for tailoring the separation factors and access to the inner catalytic zone between target molecules with identical kinetic diameter.

The alternative possibility to create hierarchic organized materials is to use protozeolitic units as zeolite seeds during the synthesis of mesoporous materials [111a], for example using solutions containing ZSM-5 precursors in the presence of a micellar template (CTACl) [111b], via the controlled coassembly of zeolitic precursors and TEOS in alkaline media [112] or using co-surfactant templating systems [113], to prepare mesoporous materials incorporating microporous units in the walls of mesoporous channels [114]. In these methods, the protozeolitic units are incorporated in the mesoporous silico-alumina (or other metal oxides) structure. However, it is also possible to directly self-assemble these protozeolitic units into macroshaped materials. For example, Zheng et al. [115] prepared mesoporous aluminosilicate ropes (fibrous morphology) with good hydrothermal stability via self-assembly of protozeolitic nanoclusters with cetyltrimethylammonium bromides (CTAB) template micelles in HNO_3 solution.

An interesting alternative to prepare metallo-silicate zeolites with fibrous morphology was shown by Park et al. [116]. Using microwave irradiation, it is possible to stack the zeolite nanocrystals, because metal ions inserted in the zeolite (Ti, in particular) act as glue between the preformed nanocrystals inducing their regular stacking to form pillars. Framework Ti species are strongly activated by microwave irradiation and lead to the formation of Ti–O–Ti and/or Ti–O–Si bonds between crystals. Fig. 4a shows the stacked morphology of Ti-silicate (MFI structure) obtained by microwave irradiation in comparison with the morphology of the same material (TS-1) obtained using conventional hydrothermal synthesis. The two samples have different catalytic behaviour.

While protozeolite units are 3D-like, a recent development of Ryoo et al. [117] was the possibility to prepare 2D-like nanosheets. The possibility of delamination (exfoliation) of some layered zeolite structures (for example, MCM-22 having MWW structure) to form zeolitic lamellas (called ITQ-2) is known from over a decade [118]. The preparation starts from a zeolite precursor for the MWW-type structure, which consists of inorganic layers connected together

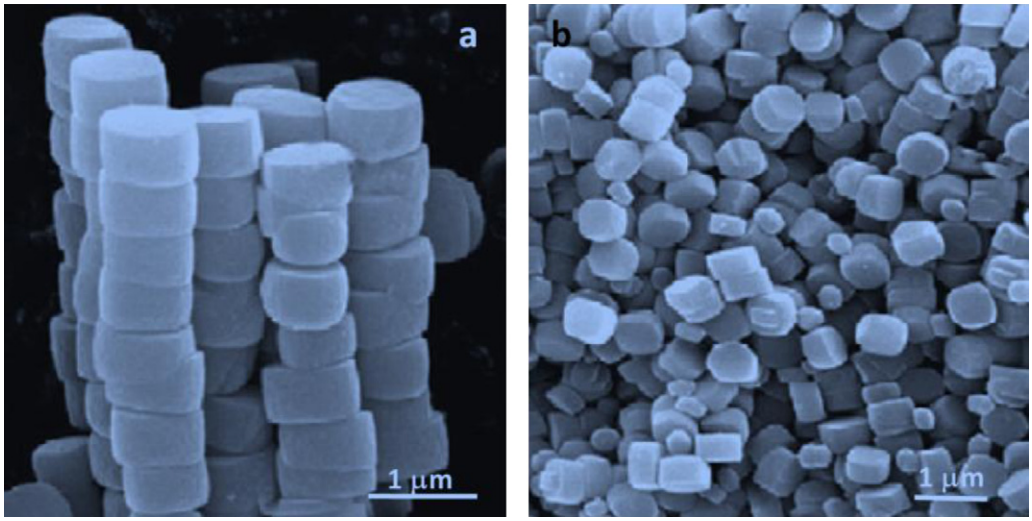

Fig. 4. Scanning electron microscopy (SEM) images showing (a) the stacked Ti-silicalite nanocrystals obtained by synthesis in the presence of microwave irradiation in comparison with the morphology obtained using conventional hydrothermal synthesis (b).
Adapted from Ref. [116a].

by a layer of organic material (hexamethyleneimine). Then the sample is swelled by refluxing with an aqueous solution of hexadecyltrimethylammonium bromide and tetrapropylammonium hydroxide. The layers are forced apart by placing the slurry in an ultrasound bath. After acidification until the pH is below 2, the solid is collected by centrifuging. Finally, the organic material is removed by calcination. The delamination of the layered precursor of the MCM-22 zeolite affords monolayers of a crystalline aluminosilicate with more than 700 $m^2\ g^{-1}$ of a well-defined external surface formed by cups of 0.7×0.7 nm (Fig. 5a). In this layered structure, the circular 10-member-ring microporous system is preserved. The resultant material presents the strong acidity and stability characteristic of the zeolites but, at the same time, offers the high accessibility to large molecules characteristic of the amorphous alumino-silicates.

The new method to produce zeolite nanosheets introduced by Ryoo et al. [117] allows instead to directly synthesize the materials. In addition, the delamination procedure is limited to few materials (in addition to ITQ-2, ITQ-6 produced starting from ferrierite), while the Ryoo's method can be used to a variety of different zeolites. Finally, a main relevant difference is that in delaminated materials the zeolite characteristic of reaction within a confined environment is essentially lost. In ITQ-2, 10-membered ring channel system is preserved, although of limited access, while the 12-membered ring is open in two cups (Fig. 5a). The Ryoo's novel procedure [117] is based on the use in the synthesis of zeolite nanosheets of a novel surfactant composed of a long-chain alkyl group (C22) and two quaternary ammonium groups spaced by a C6 alkyl linkage. The diammonium head group acted as an effective structure-directing agent for the zeolite, while the hydrophobic interaction between the long-chain tails induced the formation of a mesoscale micellar structure. With the surfactant, an ultrathin zeolite framework was formed at the hydrophilic part of the micelles while the hydrophobic tail restricted the excessive growth of zeolites.

The method was used to synthesize MFI zeolites, but other zeolitic structures can be also prepared in principle. It allows one

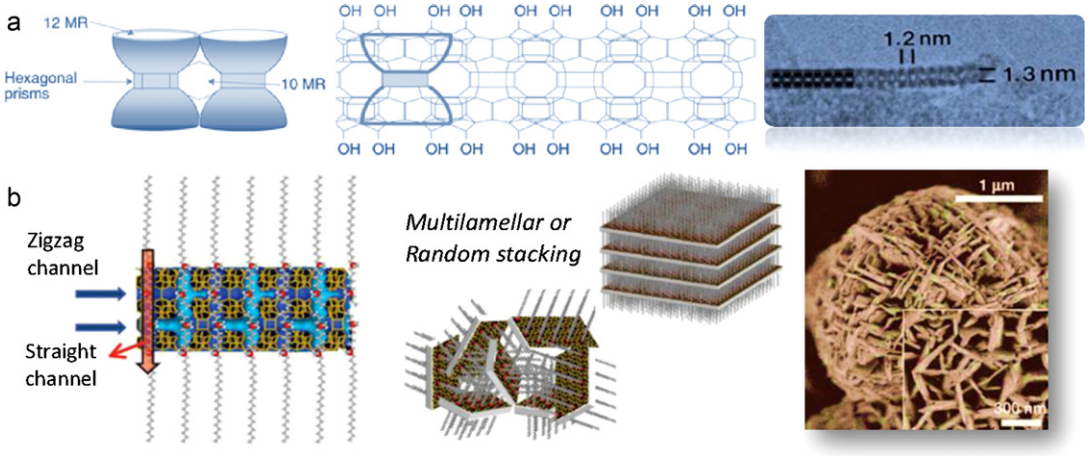

Fig. 5. (a) *Zeolite lamellas by delamination*: structure for the ITQ-2 layer showing the characteristic 10-membered ring (10 MR) separating arrays of 'chalices' perpendicular to (0 0 1), each made of two 'cups', connected by a non-shared 6-membered ring at the bottom, and with a 12-membered ring (12 MR) at their open top; transmission electron microscopy image of an 2.5-nm thick ITQ-2 layer, viewed along the 10-ring channels, perpendicular to the *c*-axis. Adapted from Ref. [118a]. (b) *Zeolite nanosheets by direct synthesis*: model for the single MFI nanosheet with the surfactant molecules aligned along the straight channel of MFI framework. Many MFI nanosheets form either multilamellar stacking along the *b*-axis, or a random assembly of unilamellar structure. SEM image shows that the MFI zeolite has a plate-like morphology that is composed of threedimensionally intergrown nanosheets.
Adapted from Ref. [117a].

to obtain zeolite nanosheets composed of alternating layers of few nm-thick zeolite framework and surfactant micelles aligned along the straight channel. The zeolite layer may be changed from 3 to 5–6 sheets and thus a true zeolite nano-environment exists (Fig. 5b). Multilamellar stacking along the *b*-axis, or a random assembly of unilamellar structure (by reducing the concentration of Na^+ in the synthesis mixture) is possible. The scanning electron image (Fig. 5b) of an as-synthesized sample indicates the presence of a desert rose-like morphology. The surface area ranges from 710 $m^2 g^{-1}$ to 520 $m^2 g^{-1}$ for the unilamellar and multilamellar nanosheets, respectively.

4.2. Nanostructured composites

The development of nanostructured composites is a different approach to design specific catalyst architecture functional to enhance the catalytic performance. An interesting possibility is to develop core–shell nano-composites. There are various industrially relevant cases when this nanostructure is advantageous. In the case of separation and storage processes using zeolite materials, for example, a core zeolite would provide high adsorption capacity and a different zeolite on the shell layer high selectivity for separation. Valtchev et al. [119] have investigated in detail these aspects.

Core–shell zeolite composites possess a core (a relatively large single-crystal) and a very thin polycrystalline shell of a different zeolite structure. The incompatibility between the core crystals and the zeolite precursor mixture yielding the shell layer can be circumvented by the adsorption of nanoseeds (protozeolites) on the core surface, which induces the crystallization of the shell. The pre-treated core crystals are subsequently subjected to a continuous growth in a zeolite precursor mixture. The feasibility of this synthetic approach has been exemplified by the preparation of core–shell β-zeolite–MFI composites [119a,c], but can be extended to other types of zeolites [119b]. Fig. 6 shows a scanning electron microscopy (SEM) image of a core–shell β-zeolite (BEA)–silicalite-1 (MFI) micro-composite. The use of a core–shell beta/silicalite-1 material allows separating mono- and dibranched paraffins with an even higher selectivity than crystals of silicalite-1 combined with the higher capacity of zeolite beta [119d]. A high selectivity in favour of the mono-branched isomers was found based on single component static adsorption, and confirmed by flow adsorption experiments using a mixture of different components.

A similar approach could be used to prepare also metal-oxide/zeolite core–shell composites. Very interesting results in this direction have been reported recently by Tsubaki et al. [120] in preparing core–shell composite catalysts with Cu–ZnO–Al_2O_3 in the core and H-ZSM-5 in the shell, in order to develop one-step direct synthesis of dimethyl ether (DME) from syn gas. The first compound is the well-established catalyst for the synthesis of methanol from syngas (CO/H_2), while the zeolite catalyst is active in the dehydration of methanol to DME, which is an acid catalysed reaction. DME is an industrially important intermediate, as well as a promising clean fuel. Its commercial synthesis occurs traditionally in two consecutive steps from syngas to methanol and then to DME. However, using a physical mixture of the two catalysts do not allow one to obtain good performance in the direct syngas to DME synthesis. Table 1 compares the catalytic performance of copper–zinc–alumina (CZA) methanol synthesis catalyst with those of a mechanical mixture of CZA and H-ZSM-5 zeolite powder (CZA-M) and of the core–shell composite catalyst with CZA as the core (millimeter-size) and H-ZSM-5 as a thin shell layer (about 5 μm) (CZA-Z). The amount of zeolite is about 8–10% wt.

The CZA is highly selective to methanol, as expected. By mixing this catalyst with H-ZSM-5 (Si/Al = 163) a mixture of methanol and DME is obtained and a slightly higher conversion of CO, because both methanol and DME syntheses are reversible reactions. The core–shell catalyst shows instead low conversion, but nearly complete selectivity to DME. The lower activity is due to the partial migration of Al (during the synthesis of the zeolite shell) to the CZA, reducing its specific activity. By reducing the amount of Al during the synthesis of the shell zeolitic layer (the Si/Al ratio in the shell increases from 32 to 221, and thus decreases the number of acid sites), the catalyst shows higher activity with respect to CZA-Z case (CO conversion of 30.4%), although the selectivity to DME is lower (78.6%), even if still better that for CZA-M sample. The results are thus still not optimal and should be further supported from more detailed catalytic studies (at equal conversion, because conversion influences the selectivity), but indicate an interesting direction to go. The interesting aspect of the core–shell structure in not only the optimized contact between the two catalysts, an important aspect in reversible consecutive reactions, but especially the better energetic integration. The methanol synthesis is exothermic, but the heat produced in the core catalyst is effectively used in situ by the DME synthesis on the zeolite shell. The fast conversion of methanol also reduces side reactions of dehydration to alkane or alkene.

Table 1
Comparison of the catalytic performances in DME direct synthesis from syngas of copper–zinc–alumina (CZA) with those of a mechanical mixture of CZA and H-ZSM-5 zeolite powder (CZA-M) and of the core–shell composite catalyst with CZA as the core and H-ZSM-5 as a thin shell layer (CZA-Z).

Catalyst	CO conv., %	Selectivity, %	Methanol	
			DME	Others
CZA	44.0	98.4	0.5	1.1
CZA-M	58.1	57.3	40.5	2.2
CZA-Z	5.6	3.4	96.6	0

Adapted from Ref. [120].
Reaction conditions: 523 K, 5.0 MPa, W_{CZA}/F_{syngas} = 10 g h mol^{-1}, syngas: $H_2/CO/CO_2/Ar$ = 59.2/32.6/5.2/2.0.

The concept of core/shell zeolite composite to improve the catalytic performance have been further applied by various other authors recently, for example to prepare improved catalysts for toluene disproportionation by making a silicalite shell over ZSM-5 extrudate [121] or for n-octane catalytic cracking by preparing core–shell Y/Beta composite [122].

A modification of the core–shell concept is to use as core a material which can be then eliminated (by combustion, selective dissolution or other methods) to form zeolite hollow spheres with a regular system of macro-cavities [123]. Fig. 7 reports the schematic draw of the process for the preparation of hollow zeolite spheres and bodies with a regular system of macro-cavities starting from polystyrene beads as shape-directing macro-templates. SEM images of the type of materials obtained after calcination is also shown.

Other type of templating materials can be used as starting point to create a specific nano-architecture. For example mesoporous carbon replica of tuneable colloidal crystals (about 10–40 nm silica nanoparticles) were employed to prepare nano-sized single-crystals silicalite-1 with ordered imprinted mesoporosity [124]. Due to the confined growth, novel crystal morphologies, consisting of faceted crystal outgrowths from primary crystalline particles were obtained. The synthesis of nano-materials within confined nanospaces (mesoporous carbon replica, carbon nanotubes, etc.) is a research area of growing interest, for the possibility to obtain unusual crystal morphologies for nanoparticles.

Hollow zeolite capsules can be prepared also by different approaches, for example by vapour-phase treatment of nanozeolite (seeds) deposited on mesoporous silica. Under the effect of the amine vapour during vapour-phase treatment, the seeds on the surface grew up by consuming the silica “nutrition” in the MS cores, and the hollow spherical shells built of grown zeolite crystals were formed upon the complete digestion of the mesoporous

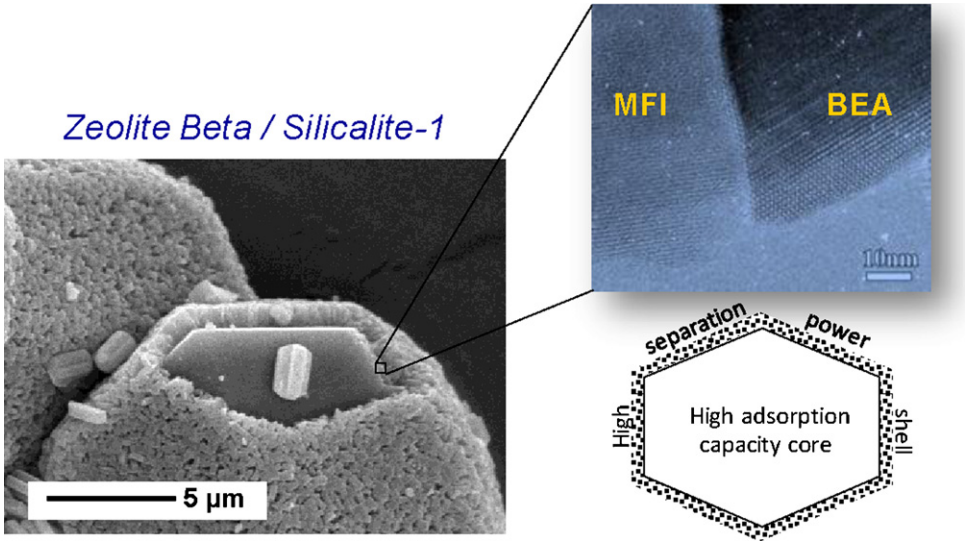

Fig. 6. SEM image of a core–shell β-zeolite (BEA)–silicalite-1 (MFI) microcomposite. In the inset, HRTEM image of the core–shell structure along the 100 direction of the BEA crystal.
Adapted from Ref. [119a].

silica spheres [125]. An interesting aspect is that it is possible to pre-incorporate in the mesopores of the silica template inorganic guests species (for example, metal nanoparticles), allowing thus to obtain directly hollow zeolite capsules containing other catalytic particles. This approach allow to develop nano-reactors based on a zeolite porous shell and catalytic elements confined inside, for example enzymes for the efficient digestion of proteins [126] or noble metals (Pt, Ag) for gas phase selective oxidation reactions [127]. Encapsulation of the metal nanoparticles in a porous hollow shell avoids their sintering, because the metal sintering is considerably inhibited. This is an area of considerable recent research interest [128,129]. The oxide shell may not only act as physical container (to avoid sintering in gas phase reactions or leaching in solution), but also as co-catalyst or to protect the inner catalyst from poisoning.

4.3. Ordered 1D-type metal oxides

Metal oxides are an important class of heterogeneous catalysts [130]. They find direct application in a variety of reaction, from acid–base to redox reactions, in photocatalytic processes, and as catalysts for environmental protection. A key aspect of metal oxides is that they possess multiple functional properties: acid–base, redox, electron transfer and transport, chemisorption by σ and π-bonding of hydrocarbons, O-insertion and H-abstraction, etc. [131]. This multi-functionality allows making selectively complex multistep transformations. For example, n-butane selective oxidation to maleic anhydride is a 14th electron oxidation involving the extraction of 8H atoms, the insertion of 3O atoms and which various different type of active sites are needed to be completed [131]. A vanadyl pyrophosphate catalyst is able to make selectively (up to over 90% selectivity) this transformation in a single step without desorption of any intermediate from the catalyst surface [132]. A main difference between heterogeneous and homogeneous catalysis is the ability of the former to make complex multistep reactions. This is an important characteristic towards developing sustainable (green) chemical processes, because the reduction of the reaction steps means a reduction of waste and energy consumption, and safer operations.

The control of the catalyst multi-functionality requires the ability to control the nanostructure and nano-architecture, i.e. the 3D spatial organization of nano-entities [131]. The previous sections have already highlighted how the nano-scale environment around the active site and the presence of nano-confinement effects are important aspects to control the catalyst reactivity, in addition to the specific nature of the active sites. Furthermore, a suitable hier-

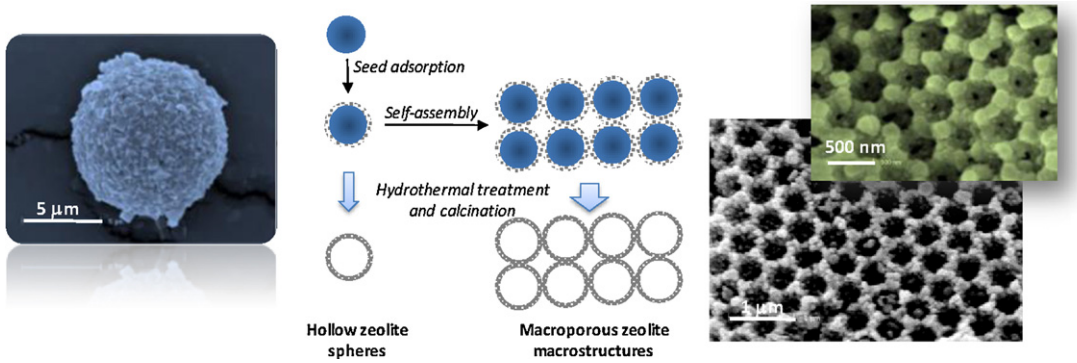

Fig. 7. Schematic representation of the process for the preparation of hollow zeolite spheres and bodies with a regular system of macrocavities starting from polystyrene beads, with SEM images of a zeolite A shell formed after the hydrothermal treatment (left figure) and of the macropore ordered structure (right figures). In the latter the walls are built of intergrown nanocrystals. The openings between the regular system of macropores are also visible.
Adapted from Ref. [123].

archic pore structure is necessary to combine a high surface area (and thus activity) with low diffusional limitations. The latter are critical not only for the reaction rate, but also for the selectivity. In consecutive reactions (the typical cases in many industrial relevant reactions) intraphase diffusional limitations would significantly decrease the selectivity of the intermediate product. Although in metal oxides catalysts the problem of designing optimal catalyst architecture has been less considered with respect to zeolite-type catalysts, above comments indicate how instead it is a critical element to improve the performance. There is also an additional aspect, which has been scarcely considered.

A recent interesting development is the possibility to monitor single-nanoparticle catalysis at single-turnover resolution using single-molecule fluorescence microscopy [133,134]. Colloidal Au nanoparticles catalyse the fluorogenic reduction of nonfluorescent resazurin to highly fluorescent resorufin by NH_2OH in aqueous solutions. By using fluorescence microscopy it is possible to have single molecule imaging of fluorescence and thus to monitor in time and space the turnover of each active site. It is thus possible to follow the single-molecule kinetics of nanoparticle catalysis [133e]. A similar method can be also used for other catalytic reactions, such as the monitoring of the epoxidation on Ti-MSM-41 catalyst [134c].

Although care should be taken in extrapolating these results, which necessarily are made in conditions far from those present during the catalytic reactions, the most outstanding observation of these experiments is that the activity with time is not constant, but a peak in activity is followed from a long time without activity. The behaviour is thus quite different from what expected for a classical kinetic mechanism of catalytic reaction such as that based on Langmuir–Hinshelwood approach [133e], neither consistent with that expected based on the sticking coefficient. This relaxation time between two consecutive reactions at the same active site is thus deriving from the catalysis-induced and spontaneous dynamic surface restructuring.

There is increasing evidence by advanced in situ studies [135–138] that a dynamic surface reconstruction of the active sites occurs in many industrial relevant reactions. Although these observations were mainly made for supported metal particles, it is reasonably expected that also occurs in metal oxides. In complex reactions, there is an exchange of many electrons and release/adsorption of significant heat of reaction. Metal oxides, although possess some electron and heat transport properties, are less effective than metals. Therefore, the relaxation time necessary to return to the initial catalyst state (both the active sites and the nano-environment) suitable to start a next reaction cycle may be long.

These observations also indicate the concept that it is necessary to turn the perspective in catalytic studies from the investigation of the reaction mechanism, i.e. the nature of the active cycle and how to accelerate the different reaction steps (in other words, the analysis of the active site turnover), to the analysis of how to accelerate the relaxation time of the active sites, i.e. the time in between two consecutive catalytic cycles in the same active site. From this perspective, the catalyst nanostructure and nano-architecture would play an important role. Nano-objects with low dimensionality, for example nano-tubes, -rods, -wires etc., would favour a faster mechanism of charge transport and dynamic of reconstruction. Carbon nanotubes and nanofibers are known to possess better electron and heat transport properties with respect to equivalent graphitic active carbon due to the better nano-order which avoid many grain and boundary interfaces. Similar effects are also expected in metal oxides [139]. Ordered metal-oxide nanostructures offer thus various potential advantages in developing advanced catalysts: (i) a higher geometrical surface area with reduced microporosity, (ii) improved electron and heat transport, (iii) possibility of nanostructuring the surface in the form of catalytic nano-reactors, and (iv) nano-confinement and 3D geometrical architectures of active sites.

Also in terms of fundamental studies, ordered metal-oxide nanostructures offer potential advantages to bridge the material gap in catalysis [140]. Most of the studies on real "nanostructured" oxides are based on materials not having a well-defined 3D structure (both short and long-range), being composed of irregularly shaped nano-crystals. These materials are polycrystalline, and show several nano-interfaces, which stabilize microstrains, oxygen vacancies or metal ions in unusual coordination states. A 3D environment for adsorption/transformation may significantly modify the adsorption of reactants and induce stabilization of transition state complexes, a well-known concept in enzymes, but typically not considered for solid catalysts. In 1D-type metal-oxide nanostructures it is instead possible to have a high local order which facilitates surface studies, but also materials suitable for applied and kinetic catalytic studies.

Low dimensional oxides are characterized by a change in the exposed crystalline planes with respect to those irregularly shaped planes present in conventional oxides and this would affect significantly their catalytic behaviour. In general, when the dimensions of a system are reduced to the nanoscale domain, the number of atoms at the surface significantly increases along with the increase in surface area per unit volume. However, this also increases the grain boundaries and the presence of defect interface sites. In metal oxides, very small nanoparticles often do not show good catalytic performance for this reason, but in 1D-type nano-oxides this phenomenon is significantly reduced. In addition, nanoparticles give an easy sintering to reduce surface free energy and defects (strain-induced grain-growth). 1D-type metal oxides show instead a higher thermal stability.

Ueda et al. [141] prepared metal oxide nanotubes with a variety of shape structures by using carbon nanofibers with different shapes as templates. The template was filled with a solution of the metal oxide precursor diluted with an organic solvent (for example, $Zr(OnPr)_4$ in C_2H_5OH, $Al(OsecBu)_3$ in CCl_4, or $SiCl_4$ in CCl_4). After removing the excess precursor solution by filtration, the samples were dried in air and the precursor was immediately hydrolyzed by the water vapour in air. Consequently, the carbon nanofiber templates were covered with a thin oxide and hydroxide. By repeating the procedure many times and finally eliminating the carbon nanofiber by calcination it is possible to obtain low dimensional metal-oxide materials as a replica of the starting 1D-type carbon template, for example oxide nanotubes with a helical structure, reflecting the shapes of starting carbon nanocoils. ZrO_2, Al_2O_3, and SiO_2 helical oxide nanotubes with various inner diameter, coil diameter, and coil pitches were produced in this way [141]. Various other oxides (Fe_2O_3, Co_3O_4, NiO) and mixed oxides ($NiFe_2O_4$, $LaMnO_3$) transition metal oxide nanotubes could be synthesized [141b].

There are various synthesis strategies to prepare 1D-type metal oxide nanomaterials (e.g., nanorods, nanowires, and nanotubes) [142,143]. Vapour phase methods, such as physical or chemical vapour phase deposition have often been used to prepare metal oxide nanorods of V, Zn, Fe, Ti and other metals [142,144,145]. The method allows one to prepare interesting materials, but it is quite expensive to prepare technical catalysts. The use of template method also allows to synthesize well defined nanostructures, but would require many steps and thus is also of difficult application. In addition to nanocarbon materials as described above, inorganic template materials, such as mesoporous silica materials or anodized aluminium oxide (AAO), could be used. This method allows one to prepare not only metal oxides, but also metal nanowires.

More interesting from the perspective of preparation of technical catalysts based on anisotropic nanocrystals are the

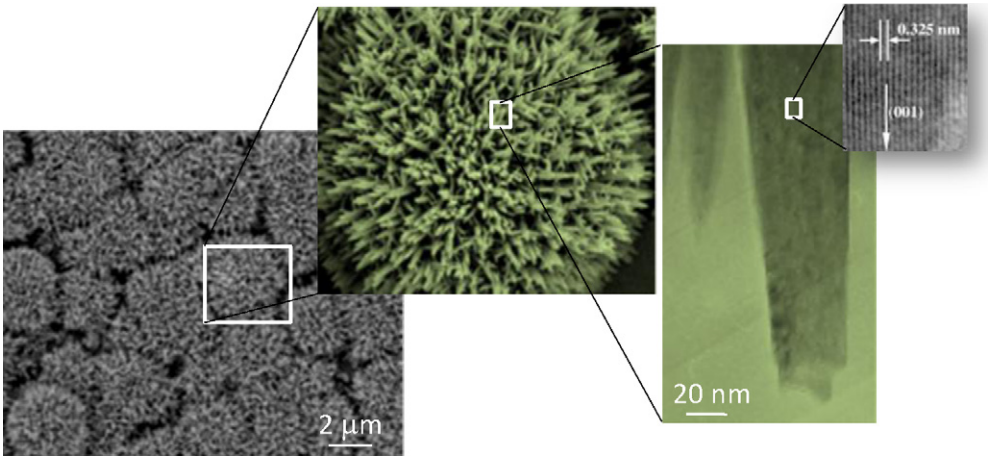

Fig. 8. FESEM image of a TiO_2 nanorod film deposited on a glass wafer with a detail of the morphology of a single papilla at high magnification, and TEM image of a single TiO_2 nanorod with a detail of the high resolution well crystalline structure (presence of clear lattice fringes parallel to the wall, with the inter-plane distance of 0.325 nm for the (1 1 0) planes perpendicular to the rod axis).
Adapted from Ref. [149].

solution-based chemical routes, because potentially less costly and easier scalable. The use of a self-assembly method is particularly interesting, and developed especially for titania materials [139]. Kasuga et al. [146] first observed that TiO_2 particles rearrange to form nanotubes with relatively small inner diameter (8 nm) and a low elongation ratio (around 10–15), e.g. the ratio between length and size of the nanotube, in NaOH concentred solution (5–10 M) under hydrothermal conditions (temperature around 110–120 °C). This study opened the investigation on this type of materials. The hydrothermal treatment of the TiO_2 crystals in alkaline environments was later modified and a simplified alkaline treatment was used for nanotube synthesis [147]. The NaOH treatment hydrolyses the Ti–O–Ti bonds between the basic octahedral building blocks in the titania structures by forming hydroxyl bridges between Ti ions, resulting in a zigzag structure. While this mechanism leads to the growth of anatase phase in [0 0 1] direction, lateral growth was found to take place under the influence of oxy bridges between titanium ions. To saturate the dangling bonds and to lower the surface energy the sheet like structures roll-up to form nanotubes [147].

Surface modified titanate sodium nanotubes ($Na_2Ti_2O_4(OH)_2$) assemble and form nanorods [148], when n-octadecyltrichlorosilane (OTS) was added to previously synthesized nanotubes dispersed in toluene. The nanorod formation can be attributed to a special packing of the surface modified nanotubes, through a hydrophobic interaction between long fatty chains. The self-assembled structure is characterized by 1 μm long nanorods that are 50–400 nm wide. The nanorods can be also assembled at the air–water interface by using the Langmuir–Blodgett technique. Titania nanorod films could be deposited on glass slides using a low temperature hydrothermal route to produce assembled nanorods having morphology similar to papillae [149] forming a micro- and nano-hierarchical architecture (Fig. 8). The papillae with 2–6 μm diameters consist of nanorods with 30–60 nm diameters.

Several methods to produce assemblies of titania nanorods or similar 1D-nanostructures have been reported recently. Lai et al. [150] reported that highly crystallized anatase TiO_2 nanorod bundles can be prepared by a hydrothermal method in the presence of tetramethylammonium hydroxide (TMAOH). TMAOH plays a structural template role to modify the TiO_2 particle shape to nanorod. The TiO_2 nanorod bundles show relatively higher photocatalytic activity than Degussa P25 evaluated via the degradation of phenol. Bahnemann et al. [151] also reported the superior photocatalytic performance of TiO_2 nanorods which could be also partly decorated with anatase nanoparticles to promote the performance. The enhanced properties are probably related to a different nature of surface hydroxyl groups in 1D-type titania materials [152]. In addition, the photocatalytic decay rate is closely related to the nanorod morphology [153].

The superior catalytic performance is thus closely related to the nanomorphology. In addition, nanorod arrays are also very suitable to develop microchannel-based microreactors for high efficient and continuous-flow photocatalysis [154] due to their characteristics. There are thus various motivations to develop these ordered 1D-type metal oxide catalysts. This is a fast growing area of research.

In various applications, it is necessary to obtain an ordered array of 1D-type nano-oxides, for example in many catalytic applications as advanced electrodes [28]. For example, dye-sensitized solar cells (DSSCs) made from oriented, one-dimensional semiconductor nanostructures such as nanorods, nanowires, and nanotubes are receiving attention because direct connection of the point of photogeneration with the collection electrode using such structures may improve the cell performance. Specifically, oriented single-crystalline TiO_2 nanorods or nanowires on a transparent conductive substrate would be necessary. A large synthesis effort was made recently to prepare this type of ordered array of 1D-type metal oxides (TiO_2 and ZnO, in particular).

Liu and Aydil [155] have used a hydrothermal method to grow oriented, single-crystalline rutile TiO_2 nanorods on a transparent conductive fluorine-doped tin oxide (FTO) substrate. An HCl aqueous solution containing titanium butoxide was used for the hydrothermal synthesis at 150 °C (20 h). The nanorods are tetragonal in shape with square top facets and are nearly perpendicular to the FTO substrate (Fig. 9a). The diameter, length, and density of the nanorods could be varied by changing the growth parameters, such as growth time, growth temperature, initial reactant concentration, acidity, and additives. The epitaxial relation between the FTO substrate and rutile TiO_2 with a small lattice mismatch plays a key role in driving the nucleation and growth of the rutile TiO_2 nanorods on FTO. A similar method was reported by Guo et al. [156] to prepare well-aligned TiO_2 nanorod arrays on pretreated quartz substrates via a hydrothermal method and by Tao et al. [157] to prepare oriented single crystalline TiO_2 nano-pillar arrays on a Ti substrate in tetramethylammonium hydroxide (TMAOH) solution by a one-pot hydrothermal method. The TiO_2 nano-pillars are characterized by a tetrahydral bipyramidal tip growing vertically on the titanium substrate.

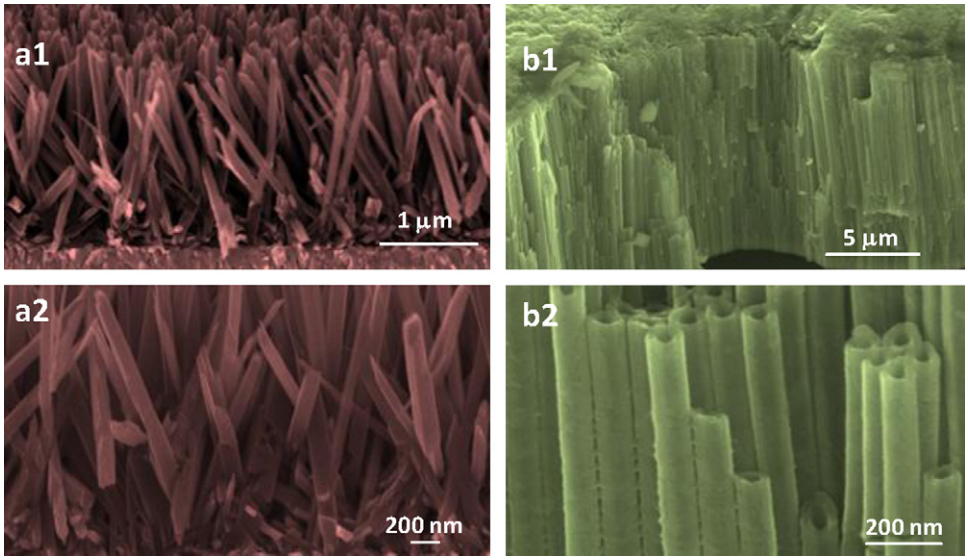

Fig. 9. (a) FESEM images of an oriented rutile TiO2 nanorod film grown on FTO substrate (150 °C for 20 h). The average diameter and length are 90 ± 5 nm and 1.9 ± 0.1 μm, respectively. Adapted from Ref. [155]. (b) FESEM images (cross section) of nanotube arrays obtained by anodic oxidation of a Ti foil in ethylene glycol containing NH4F applying a 50 V potential for 6 h. The thickness of the titania nanostructured film is about 15 μm; tube internal diameter is 40–43 nm while tube external diameter is in the range 100–105 nm.
Adapted from Ref. [160].

An alternative attractive method to produce dense arrays of titania nanotubes is by anodic oxidation [158,159]. The method is based on the electrochemical self-assembly of titania nanotube arrays during the anodic oxidation of Ti foils or thin layers. A thin layer of oxide forms initially during the anodization process due to exposure of the Ti metal to the acidic electrolyte. Small pits originate in this oxide layer due to the localized dissolution of the oxide, making the barrier layer at the bottom of the pits relatively thin which, in turn, increases the electric field intensity across the remaining barrier layer. The increase in electric field enhances electrochemical dissolution resulting in further pore growth, leaving un-anodized metal portions between the pores. As the pores grow deeper the electric field in these metallic regions increases, enhancing field-assisted oxide growth and oxide dissolution, hence simultaneously with the pores well-defined inter-pore voids start forming. After this, the nanotubes and voids grow in equilibrium and the nanotube length increases until the electrochemical etching rate equals the chemical dissolution rate at the top surface. A precisely controlled rate of chemical dissolution of the metal or oxide by the acidic electrolyte in the presence of an electric field plays a key role in the formation of the nanotube arrays rather than a nanoporous structure.

The first generation of nanotube array was prepared using aqueous electrolytes, and then the procedure improved by using polar organic electrolytes [158b]. Using the latter electrolyte, in particular ethylene glycol (EG), very thick films up to over 150 μm could be obtained (Fig. 9b). The control of the various parameters allows one to obtain very precise control in the characteristics of the nanotubes (diameter, thickness of the walls, array density, and morphology of the nanotubes). In all these procedures, fluoride ions were used to dissolve the oxide, but recently fluoride free electrolytes were also used. The characteristics of the nanotube array obtained by anodic oxidation are very different from those obtained by hydrothermal methods. Fig. 9 compares the films obtained by the hydrothermal method used by Liu and Aydil [155] with those obtained by anodic oxidation using EG as electrolyte [160]. The latter allows a more dense packing and well ordering/alignment of titania nanotubes, with better light harvesting and efficient photo-behaviour.

The control of the anodization parameters and particularly of the rate of electrochemical dissolution leads to complete anodization of a Ti foil, resulting in a free-standing nanotube array membrane [161] of thickness 100–200 μm. Maximum nanotube packing density and membrane thickness was achieved using EG as the electrolyte. The nanotube coordination number is usually six, i.e. each nanotube is surrounded by six others, with strong bonding between adjacent tubes. This structure allows one to obtain membranes of uniform pore size suitable for use in filtration applications [161–163]. Usually, to prepare the membrane it is necessary to preliminary protected with a polymer one side of a Ti foil. After anodization, the resulting nanotube array film can be separated from the underlying Ti substrate by dipping the sample in ethyl alcohol followed by ultrasonic treatment to separate the nanotube array film. The membranes are flat while wet, but curl when dried in air leading to possibly breaking. This is due to the surface tension forces of the solution acting on the membrane. Rinsing with low surface tension liquids facilitates to obtain flat membrane after drying. Alternatively, critical point drying can be used in which the membrane flatness is preserved. To open the closed bottoms of the freestanding nanotube layer, the wet nanotube film may be exposed for 30 min to HF vapours. This procedure leads to preferential HF gas condensation at the tube bottoms causing etching of the backside layer.

It is thus possible to obtain by this procedure nano-membranes with thickness of about 100–200 μm and uniform straight channels of about 50–100 nm. An interesting perspective application is to develop novel nano-reactor concepts. Micro-reactor technology and catalysis are two of the crucial pillars to foster a sustainable industrial chemistry [6]. There are several examples, which show their critical role to achieve more eco-efficient chemical syntheses and develop processes with high resource efficiency and reduced amounts of waste and/or emissions. They are key components of process intensification, i.e. to pass from energy- and capital-intensives to safer and eco-friendly processes, with a positive impact also on the competitiveness of the chemical industry. Usually, micro-reactors have channels in the micrometer diameter range (around 100–150 μm), but the passage from micro- to nano-reactor would bring several benefits. It would further increase the possible process intensification by one-two orders of magnitude, and significantly improve safety. It is known that the higher wall-to-volume ratio in micro-reactors with respect to conventional

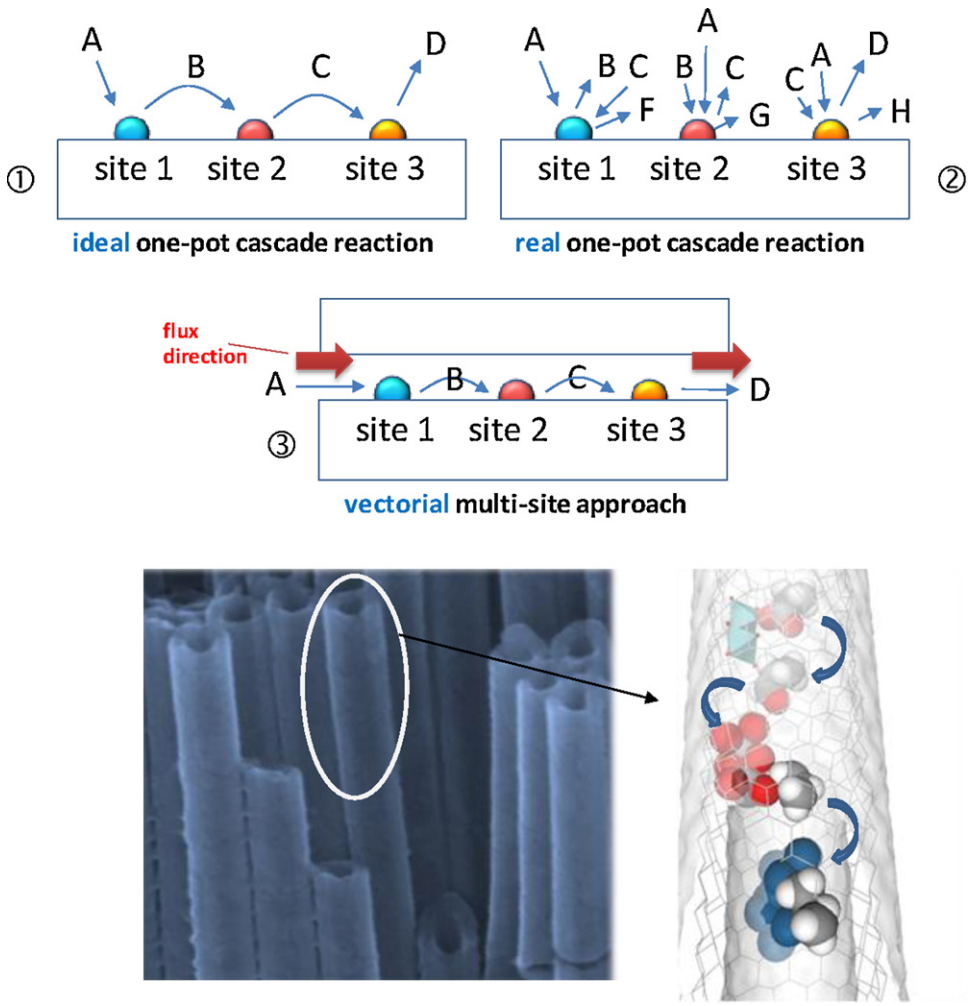

Fig. 10. Concept of vectorializing the active site sequence in complex, multistep reactions. On the top: (1) One-pot ideal cascade reaction versus (2) real case, and (3) proposed concept of vectorial multi-site approach in the nanopores of a membrane. On the bottom: SEM image of a titania nanomembrane produced by anodic oxidation and pictorial view of multisite catalytic sequence confined within one channel of the nanomembrane.

reactors, allows one to effectively quench radical-type reactions and runaway effects. In nano-reactors, the further increase of one-two order of magnitude in the wall-to-volume ratio will further increase safety of operations, allowing, for example, operating without risks inside the explosion region, or with highly exothermic reactions. Interestingly, they offer the opportunity to vectorialize the active site sequence in complex, multistep reactions.

The optimization of the use of resources and energy, e.g. improve atom-economy and selectivity in complex multistep reactions, requires a novel catalyst design to control and force along a specific route the sequence of reaction steps in solventless catalytic transformations. We may distinguish two classes of catalysts. Few of them are selective in complex multistep reactions, as the already cited example of the industrial process of n-butane selective oxidation to maleic anhydride on $(VO)_2P_2O_7$ catalysts [131,132]. However, it is still not possible to design ad hoc a catalyst selective in this type of complex reactions. The second class of materials is catalysts, homogeneous or heterogeneous, able to perform selectively a single-type of reaction. To perform multi-step reactions, one-pot cascade or domino approaches are used [164,165]. This approach is important to develop next-generation catalysis for renewables [166] and to exploit the synergies between heterogeneous and homogeneous catalysis [167].

In cascade/domino catalytic approaches, different catalytic components are present (multi active sites) and the molecule is converted to the final product passing from one site to the other. In some cases, this approach was successful, but it is not possible to determine the sequence of interaction of the molecules with the active sites, because it is essentially a random interaction (Fig. 10). Therefore, the approach can be successful only when a specific one-to-one interaction is present, e.g. the reactant and intermediates react only with one specific site. To overcome this problem and generalize the approach, it is necessary to force the sequence of steps of reaction. We define this as vectorial multi-site approach (Fig. 10). To have a vectorial multi-site approach the random diffusion path should be shorter with respect to a vectorial driving force related to a 1D flux. If the sequence of sites is localized in an ordered manner inside a 1D channel and a gradient is applied along the axial direction to force the flux, it is thus possible to realize a controlled reaction sequence close to the ideal situation. However, the diameter of the channels should be of nanometric scale to realize this concept and avoid phenomena of micro-mixing.

5. Conclusions and outlooks

The last decade has significantly turned out the perspective for research and development in catalysis. From one side there are many new challenges for catalysis, from the conversion of biorenewable feedstocks [168,169] to the exploitation of less used fossil fuel resources [169,170] and the chemical exploitation of

solar energy [171,172]. From the other side, a significant progress has been observed both in tools for understanding catalysis, from in situ/operando methods [173–175] to theoretical modelling [176–178] and in synthesis methodologies to prepare tailored catalytic nanostructure. This review has analysed some of the possibilities and new trends, although the aim was not a comprehensive analysis, but to give a glimpse into this fast growing research area.

It may be noted, however, that the use of the new nano-materials as catalysts has progressed much less than the synthesis and often a clear general strategy was missing. We have analysed here some of the opportunities offered from a tailored nano-design of the catalysts, from exploiting nano-confinement effects and supramolecular active sites synergies in nano-reactors to the new possibilities offered from new concepts such as the reduction of the relaxation time between two consecutive turnover cycles on a single active site and forcing a vectorial active site sequence in complex, multistep reactions. There are some concepts, which may be considered well established, but which still need active research to be further exploited, such as the development of (i) hierarchic pore structure to maximize catalyst effectiveness [101–104] and (ii) metal complexes confined within solid cavities acting as nano-reactors [179]. New developments in nano-materials offer novel perspectives in all these areas, and in particular to develop new catalysts able to perform more selectively complex multistep reactions. This is a critical objective to improve the sustainability of various industrial chemical processes, because the reduction in the number of operations and an increase of the overall selectivity determines a lowering of energy and raw material resources, a reduction of waste, and often an improvement of safety, besides to improve process economics.

The availability of conceptually new catalysts also offers the possibility to reconsider well-established processes. It is possible to further improve the performance or redesign the process from a novel perspective previously impossible due to the lack of catalysts. Reducing energy intensity in many chemical processes is an actual issue, which should be addressed from this new perspective. For example, light olefins (ethylene and propylene) are the building bricks of petrochemistry, but their production is the single most energy-consuming process in the chemical industry. Steam cracking in year 2008 accounted for about 3 EJ (E for Exa, e.g. 10^{18}) primary energy use (due to the combustion of fossil fuels and excluding the energy content of products) and nearly 200 million tons of CO_2 emissions due to the combustion of fossil fuels [180]. The pyrolysis section of a naphtha steam cracker alone consumes approximately 65% of the total process energy and approximately 75% of the total exergy loss. Approximately 20–30% savings on the current average process-energy use are possible by using alternative processes in olefin production, e.g. catalytic dehydrogenation (DH) or oxidative dehydrogenation (ODH) of light alkanes. DH is an endothermic reversible reaction and thus it is necessary to operate at high temperature (usually above 650 °C) to have enough conversion, which is limited from equilibrium. This requires one to supply energy at high temperature (an inefficient process) and enhances the side reaction of formation of carbonaceous species over the catalyst, thus making necessary a periodic regeneration of the catalyst. By shifting the equilibrium using a catalytic membrane, it is possible to operate at lower temperature in conditions more favourable for an efficient heat transfer, which avoids the deactivation. The same concept can be applied in other energy-intensive large-scale processes, such as H_2 production by steam reforming and catalytic syngas production [181]. ODH reaction is instead an exothermic reaction not limited from equilibrium, but suffering from low selectivity due to the easy further conversion of the alkenes formed to carbon oxides. Recent results [182] showed that sub-nanometric Pt clusters (8–10 atoms) are 40–100 times more active and highly selective in the conversion of propane to propylene. The problem is to stabilize these nano-clusters in industrially relevant reaction conditions. This example shows that even for well-established and large-scale reactions there is the need to introduce next-generation catalysts based on a better nano-design. The development of novel energy-efficient solutions using alternative raw materials such as light alkanes is a relevant sustainable chemistry target [5].

The use of micro-reactors or new generation nano-reactors as shortly discussed in the previous section, is a further relevant direction to implement process intensification, reducing the use of resources and improving safety, but also offering new business opportunities [5]. There is the need of conceptually new nano-designed catalysts to realize this opportunity. As commented for nano-reactors, they also offer new possibilities to realize in one-step complex, multistep reactions.

It is necessary to push these research directions and to develop a more general strategy for the design of next-generation nano-catalysts based on understanding of the relationship between nanostructure and catalytic performance. Creating and mastering nano-objects is the direction to foster for the design of advanced catalytic materials.

References

[1] Chemicals Week, Chemical Futures: The Industry in 2020, vol. 168, no. 18, 2006, pp. 19–26.
[2] K. Heinzelbecker, J. Bus. Chem. 2 (1) (2005) 37–53.
[3] (a) Looking at the next decade: innovation and sustainability, Cefic Review 2008–2009. Available from: http://www.cefic.be (Aug. 2010).;
(b) KPMG International, The Future of the European Chemical Industry, Jan. (2010). Available from: http://www.cefic.be (Aug. 2010).
[4] Sustainable chemistry: a catalyst for innovation & growth in Europe, prepared by European Technology Platform on Sustainable Chemistry. Available from: http://www.suschem.org (Aug. 2010).
[5] (a) F. Cavani, G. Centi, S. Perathoner, F. Trifirò, Sustainable Industrial Chemistry – Principles, Tools and Industrial Examples, Wiley-VCH, Weinheim, Germany, 2009;
(b) G. Centi, S. Perathoner, Top. Catal. 52 (8) (2009) 948–961.
[6] (a) D.M. Alonso, J.Q. Bond, J.A. Dumesic, Green Chem. 12 (2010) 1493–1513;
(b) D.A. Simonetti, J.A. Dumesic, Catal. Rev.: Sci. Eng. 51 (3) (2009) 441–484;
(c) D.A. Simonetti, J.A. Dumesic, ChemSusChem 1 (8–9) (2008) 725–733;
(d) J.N. Chheda, G.W. Huber, J.A. Dumesic, Angew. Chem. Int. Ed. 46 (38) (2007) 7164–7183;
(e) Y. Roman-Leshkov, C.J. Barrett, Z.Y. Liu, J.A. Dumesic, Nature 447 (7147) (2007) 982–985;
(f) G.W. Huber, J.N. Chheda, C.J. Barrett, J.A. Dumesic, Science 308 (5727) (2005) 1446–1450.
[7] G. Centi, R.A. van Santen, Catalysis for Renewables, Wiley-VCH, Weinheim, Germany, 2007.
[8] K.E. Geckeler, H. Nishide, Advanced Nanomaterials, Wiley-VCH, Weinheim, Germany, 2010.
[9] J. Garcia-Martinez, Nanotechnology for the Energy Challenge, Wiley-VCH, Weinheim, Germany, 2010.
[10] (a) H. Liang, Y. He, Y. Ye, X. Xu, F. Cheng, W. Sun, X. Shao, Y. Wang, J. Li, K. Wu, Coord. Chem. Rev. 253 (23–24) (2009) 2959–2979;
(b) L. Qi, Coord. Chem. Rev. 254 (9–10) (2010) 1054–1071.
[11] (a) T. Valdes-Solis, A.B. Fuertes, Mater. Res. Bull. 41 (12) (2006) 2187–2197;
(b) H. Yang, D. Zhao, J. Mater. Chem. 15 (12) (2005) 1217–1231.
[12] (a) C. Yan, J. Liu, F. Liu, J. Wu, K. Gao, D. Xue, Nanoscale Res. Lett. 3 (12) (2008) 473–480;
(b) F. Liu, D. Xue, Mater. Res. Bull. 45 (3) (2010) 329–332.
[13] (a) H. Chu, L. Wei, R. Cui, J. Wang, Y. Li, Coord. Chem. Rev. 254 (9–10) (2010) 1117–1134;
(b) R. Ryoo, S.H. Joo, Stud. Surf. Sci. Catal. 148 (2004) 241–261.
[14] (a) C. Wu, Y. Xie, J. Nanosci. Nanotechnol. 8 (12) (2008) 6208–6222;
(b) C. Wu, Y. Xie, Chem. Commun. (2009) 5943–5957.
[15] Y. Zhao, L. Jiang, Adv. Mater. 21 (36) (2009) 3621–3638.
[16] (a) D.R. Rolison, J.W. Long, J.C. Lytle, A.E. Fischer, C.P. Rhodes, T.M. McEvoy, M.E. Bourg, Al.M. Lubers, Chem. Soc. Rev. 38 (1) (2009) 226–252;
(b) D.R. Rolison, Science 14 (299) (2003) 1698–1701;
(c) M.S. Doescher, J.J. Pietron, B.M. Dening, J.W. Long, C.P. Rhodes, C.E. Edmondson, D.R. Rolison, Anal. Chem. 77 (24) (2005) 7924–7932;
(d) C. Laberty-Robert, J.W. Long, K.A. Pettigrew, R.M. Stroud, D.R. Rolison, Adv. Mater. 19 (2007) 1734–1739.
[17] J.J. Pietron, R.M. Stroud, D.R. Rolison, Nano Lett. 2 (5) (2002) 545–549.
[18] W. Deng, A.I. Frenkel, R. Si, M. Flytzani-Stephanopoulos, J. Phys. Chem. C 112 (2008) 12834–12840.

[19] H. Abe, Y. Miyamoto, M. Umetsu, T. Uchikoshi, T. Okubo, M. Naito, Y. Hotta, T. Kasuga, A. Suda, M. Mori, in: M. Hosokawa, K. Nogi, M. Naito, T. Yokoyama (Eds.), Nanoparticle Technology Handbook, vol. 177, Elsevier Science Pub., Amsterdam, 2007, pp. 179–265.
[20] K. Zhu, D. Wang, J. Liu, Nano Res. 2 (1) (2009) 1–29.
[21] M.V. Landau, L. Vradman, in: V. Valtchev, S. Mintova, M. Tsapatsis (Eds.), Ordered Porous Solids, Elsevier Science Pub., Amsterdam, 2009, pp. 693–724.
[22] (a) A.-H. Lu, F. Schüth, C. R. Chim. 8 (3–4) (2005) 609–620;
(b) A. Taguchi, F. Schüth, Micropor. Mesopor. Mater. 77 (1) (2005) 1–45.
[23] M.V. Landau, L. Vradman, A. Wolfson, P.M. Rao, M. Heskowitz, C. R. Chim. 8 (3–4) (2005) 679–691.
[24] F. Fajula, A. Galarneau, F. Di Renzo, Micropor. Mesopor. Mater. 82 (3) (2005) 227–239.
[25] M. Antonietti, G.A. Ozin, Chem. Eur. J. 10 (2004) 28–41.
[26] J.M. Thomas, J.C. Hernandez-Garrido, R. Raja, R.G. Bell, Phys. Chem. Chem. Phys. 11 (16) (2009) 2799–2825.
[27] F. Zaera, J. Phys. Chem. Lett. 1 (3) (2010) 621–627.
[28] G. Centi, S. Perathoner, Eur. J. Inorg. Chem. (26) (2009) 3851–3878.
[29] N.R. Shiju, V.V. Guliants, Appl. Catal. A: Gen. 356 (1) (2009) 1–17.
[30] H.J. Freund, Chem. Eur. J. 16 (31) (2010) 9384–9397.
[31] R. Schlögl, S.B. Abd Hamid, Angew. Chem. Int. Ed. 43 (13) (2004) 1628–1637.
[32] R.T. Vang, S. Wendt, F. Besenbacher, in: A.V. Narlikar, Y.Y. Fu (Eds.), Oxford Handbook of Nanoscience and Technology, vol. 3, Oxford Univ. Press, New York, US, 2010, pp. 416–473.
[33] J.T. Thomas, ChemCatChem 2 (2) (2010) 127–132.
[34] A. Thomas, M. Driess, Angew. Chem. Int. Ed. 48 (11) (2009) 1890–1892.
[35] Z. Wang, G. Chen, K. Ding, Chem. Rev. 109 (2) (2009) 322–359.
[36] A. Corma, H. Garcia, Top. Catal. 48 (1–4) (2008) 8–31.
[37] M. Tada, Y. Iwasawa, Yasuhiro, Coord. Chem. Rev. 251 (21–24) (2007) 2702–3271.
[38] G. Centi, S. Perathoner, Catal. Today 138 (1–2) (2008) 69–76.
[39] J.M. Basset, R. Ugo, in: J.M. Basset, R. Psaro, D. Roberto, R. Ugo (Eds.), Modern Surface Organometallic Chemistry, Wiley-VCH, Weinheim, Germany, 2009, pp. 1–21.
[40] R.A. Sheldon, I.W.C.E. Arends, H.E.B. Lempers, Catal. Today 41 (4) (1998) 387–407.
[41] C.W. Jones, M.W. McKittrick, J.V. Nguyen, K. Yu, Top. Catal. 34 (1–4) (2005) 67–76.
[42] V. Dal Santo, F. Liguori, C. Pirovano, M. Guidotti, Molecules 15 (2010) 3829–3856.
[43] J. Bluemel, Coord. Chem. Rev. 252 (21 + 22) (2008) 2410–2423.
[44] J.M. Thomas, R. Raja, Acc. Chem. Res. 41 (6) (2008) 708–720.
[45] K. Ariga, A. Vinu, J.P. Hill, T. Mori, Coord. Chem. Rev. 251 (21–24) (2007) 2562–2591.
[46] F. Averseng, M. Vennat, M. Che, in: G. Ertl, H. Knözinger, F. Schüth, J. Weitkamp (Eds.), Handbook of Heterogeneous Catalysis, vol. 1, 2nd edition, Wiley-VCH, Weinheim, Germany, 2008, pp. 522–539.
[47] J. Wei, C.A. Floudas, C.E. Gounaris, G.A. Somorjai, Catal. Lett. 133 (1–2) (2009) 234–241.
[48] J. Cejka, A. Corma, S. Zones (Eds.), Zeolites and Catalysis, Wiley-VCH, Weinheim, Germany, 2010.
[49] B. Smit, T.L.M. Maesen, Nature 451 (2008) 671–678.
[50] J. Yu, R. Xu, J. Mater. Chem. 18 (34) (2008) 4021–4030.
[51] G. Centi, F. Cavani, F. Trifirò, Selective Oxidation by Heterogeneous Catalysis, Kluwer Academic Publishers, New York, 2001.
[52] E. Jorda, A. Tuel, R. Teissier, J. Kervenal, Chem. Commun. 1775 (1995).
[53] F. Schwertfeger, W. Glaubitt, U. Schubert, J. Non-Cryst. Solids 145 (1992) 85.
[54] H. Kochkar, F. Figueras, J. Catal. 171 (1997) 420.
[55] E.E. Santiso, M.K. Kostov, A.M. George, M.B. Nardelli, K.E. Gubbins, Appl. Surf. Sci. 253 (13) (2007) 5570–5579.
[56] C. Li, H. Zhang, D. Jiang, Q. Yang, Chem. Commun. (6) (2007) 547–555.
[57] F. Goettmann, C. Sanchez, J. Mater. Chem. 17 (1) (2007) 24–30.
[58] D. Lesthaeghe, V. Van Speybroeck, M. Waroquier, Phys. Chem. Chem. Phys. 11 (26) (2009) 5222–5226.
[59] (a) F. Marquez, H. Garcia, E. Palomares, L. Fernandez, A. Corma, J. Am. Chem. Soc. 122 (27) (2000) 6520–6652;
(b) F. Marquez, C. Zicovich-Wilson, A. Corma, E. Palomares, H. Garcia, J. Phys. Chem. B 105 (41) (2001) 9973–9979;
(c) G. Sastre, A. Corma, J. Mol. Catal. A: Chem. 305 (1–2) (2009) 3–7.
[60] E.G. Derouane, J. Mol. Catal. A: Chem. 134 (1–3) (1998) 29–45.
[61] Z. Blum, S.T. Hyde, B.W. Ninham, J. Phys. Chem. 97 (1993) 661–665.
[62] J.K. Thomas, Int. J. Photoenergy 4 (1) (2002) 27–33.
[63] (a) N. Tanchoux, P. Trens, D. Maldonato, F. Di Renzo, F. Fajula, Colloids Surf. A 246 (1–3) (2004) 1–8;
(b) N. Tanchoux, S. Pariente, P. Trens, F. Fajula, J. Mol. Catal. A: Chem. 305 (1–2) (2009) 8–15.
[64] J.-P. Korb, S. Xu, F. Cros, L. Malier, J. Jonas, J. Chem. Phys. 107 (10) (1997) 4044–4050.
[65] F. Cros, J.-P. Korb, L. Malier, Langmuir 16 (26) (2000) 10193–10197.
[66] T. Takamuku, H. Maruyama, S. Kittaka, S. Takahara, T. Yamaguchi, J. Phys. Chem. B 109 (2) (2005) 892–899.
[67] R. Guegan, D. Morineau, C. Alba-Simionesco, Chem. Phys. 317 (2–3) (2005) 236–244.
[68] M.S. Schneider, J.-D. Grunwaldt, A. Baiker, Langmuir 20 (7) (2004) 2890–2899.
[69] R. Gounder, E. Iglesia, Angew. Chem. Int. Ed. 49 (2010) 808–811.
[70] C. Cottin-Bizonne, C. Barentin, E. Charlaix, L. Bocquet, J.-L. Barrat, Eur. Phys. J. E: Soft Matter 15 (4) (2004) 427–438.
[71] P.E. de Jongh, P. Adelhelm, ChemSusChem 3 (12) (2010) 1332–1348.
[72] (a) W.T.S. Huck, Chem. Commun. (2005) 4143–4148;
(b) Y. Wu, G. Cheng, K. Katsov, S.W. Sides, J. Wang, J. Tang, G.H. Fredrickson, M. Moskovits, G.D. Stucky, Nat. Mater. 3 (2004) 816–822.
[73] (a) X. Pan, X. Bao, Chem. Commun. (47) (2008) 6271–6281;
(b) J. Sun, X. Bao, Chem. Eur. J. 14 (25) (2008) 7478–7488;
(c) X. Pan, Z. Fan, W. Chen, Y. Ding, H. Luo, X. Bao, Nat. Mater. 6 (7) (2007) 507–511.
[74] W. Chen, X. Pan, M.G. Willinger, D.S. Su, X. Bao, J. Am. Chem. Soc. 128 (10) (2006) 3136–3137.
[75] W. Chen, Z. Fan, X. Pan, X. Bao, J. Am. Chem. Soc. 130 (29) (2008) 9414–9419.
[76] J. Guan, X. Pan, X. Liu, X. Bao, J. Phys. Chem. C 113 (52) (2009) 21687–22169.
[77] G. Centi, S. Perathoner, Catal. Today 150 (1–2) (2010) 151–162.
[78] P. Serp, E. Castillejos, ChemCatChem 2 (1) (2010) 41–47.
[79] (a) G.A. Somorjai, F. Tao, J.Y. Park, Top. Catal. 47 (1–2) (2008) 1–14;
(b) G.A. Somorjai, J.Y. Park, Chem. Soc. Rev. 37 (10) (2008) 2155–2162.
[80] T.V.W. Janssens, B.S. Clausen, B. Hvolbaek, H. Falsig, C.H. Christensen, T. Bligaard, J.K. Norskov, Top. Catal. 44 (1–2) (2007) 15–26.
[81] (a) Y. Yao, Q. Fu, Z. Wang, D. Tan, X. Bao, J. Phys. Chem. C 114 (40) (2010) 17069–17079;
(b) Q. Fu, W.-X. Li, Y. Yao, H. Liu, H.-Y. Su, D. Ma, X.-K. Gu, L. Chen, Z. Wang, H. Zhang, B. Wang, X. Bao, Science 328 (5982) (2010) 1141–1144.
[82] V. Chechik, Ann. Rep. Prog. Chem. Sect. B: Org. Chem. 104 (2008) 331–348.
[83] I. McCort-Tranchepain, M. Petit, P.I. Dalko, in: P.T. Anastas, R.H. Crabtree (Eds.), Handbook of Green Chemistry: Green Catalysis, vol. 1, Wiley-VCH, Weinheim, Germany, 2009, pp. 255–318.
[84] G. Centi, S. Perathoner, Micropor. Mesopor. Mater. 107 (1–2) (2008) 3–15.
[85] K. Motokura, N. Fujita, K. Mori, T. Mizugaki, K. Ebitani, K. Kaneda, J. Am. Chem. Soc. 127 (27) (2005) 9674–9675.
[86] G. Astray, A. Cid, I. Garcia-Rio, P. Hervella, J.C. Mejuto, M. Perez-Lorenzo, Prog. React. Kinet. Mech. 33 (1) (2008) 81–97.
[87] D.C. Crans, B. Baruah, A. Ross, N.E. Levinger, Coord. Chem. Rev. 253 (17–18) (2009) 2178–2185.
[88] D.E. Moilanen, N.E. Levinger, D.B. Spry, M.D. Fayer, J. Am. Chem. Soc. 129 (46) (2007) 14311–14318.
[89] (a) Z. Chen, Z.M. Cui, F. Niu, L. Jiang, W.G. Song, Chem. Commun. 46 (35) (2010) 6524–6526;
(b) M.A. Mahmoud, F. Saira, M.A. El-Sayed, Nano Lett. 10 (9) (2010) 3764–3769.
[90] (a) M. Yoshizawa, T. Kusukawa, M. Fujita, S. Sakamoto, K. Yamaguchi, J. Am. Chem. Soc. 123 (43) (2001) 10454–10459;
(b) M. Yoshizawa, Y. Takeyama, T. Kusukawa, M. Fujita, Angew. Chem. Int. Ed. 41 (8) (2002) 1347–1349;
(c) M. Yoshizawa, M. Fujita, Pure Appl. Chem. 77 (7) (2005) 1107–1112.
[91] T.S. Koblenz, J. Wassenaar, J.N.H. Reek, Chem. Soc. Rev. 37 (2) (2008) 247–262.
[92] D.M. Vriezema, M.C. Aragones, J.A.A.W. Elemans, J.J.L.M. Cornelissen, A.E. Rowan, R.J.M. Nolte, Chem. Rev. 105 (2005) 1445–1489.
[93] A. Cavarzan, G. Bianchini, P. Sgarbossa, L. Lefort, S. Gladiali, A. Scarso, G. Strukul, Chem. Eur. J. 15 (32) (2009) 7930–7939.
[94] J.S. Milano-Brusco, H. Nowothnick, M. Schwarze, R. Schomcker, Ind. Eng. Chem. Res. 49 (3) (2010) 1098–1104.
[95] (a) A.K. Ganguli, T. Ahmad, S. Vaidya, J. Ahmed, Pure Appl. Chem. 80 (11) (2008) 2451–2477;
(b) I. Beletskaya, V. Tyurin, Molecules 15 (2010) 4792–4814.
[96] (a) A.K. Diallo, C. Ornelas, L. Salmon, J. Ruiz Aranzaes, D. Astruc, Angew. Chem. Int. Ed. 46 (45) (2007) 8644–8648;
(b) D. Astruc, Tetrahedron: Asymmetr. 21 (9–10) (2010) 1041–1054;
(c) A.K. Diallo, E. Boisselier, L. Liang, J. Ruiz, D. Astruc, Chem. Eur. J. 16 (39) (2010) 11832–11835.
[97] E.A. Karakhanov, A.L. Maximov, V.A. Skorkin, A.V. Zolotukhina, A.S. Smerdov, A.Yu. Tereshchenko, Pure Appl. Chem. 81 (11) (2009) 2013–2023.
[98] (a) G.E. Oosterom, J.N.H. Reek, P.C.J. Kamer, P.W.N.M. van Leeuwen, Angew. Chem. Int. Ed. 40 (2001) 1828–1849;
(b) H. Brunner, J. Organomet. Chem. 500 (1995) 39–46.
[99] Z. Bai, T.P. Lodge, J. Am. Chem. Soc. 132 (45) (2010) 16265–16270.
[100] (a) G. Centi, S. Perathoner, CATTECH 7 (3) (2003) 78–89;
(b) G. Centi, S. Perathoner, Catal. Today 79–80 (2003) 3–13.
[101] M.-O. Coppens, G. Wang, in: U.S. Ozkan (Ed.), Design of Heterogeneous Catalysts: New Approaches based on Synthesis, Characterization and Modeling, Wiley-VCH, Weinheim, Germany, 2009, pp. 25–58.
[102] P.J. Kooyman, Stud. Surf. Sci. Catal. 174A (2008) 91–99.
[103] Y. Zhang, N. Ren, Y. Tang, in: V. Valtchev, S. Mintova, M. Tsapatsis (Eds.), Ordered Porous Solids, Elsevier Science Pub., Amsterdam, The Netherlands, 2008, pp. 441–475.
[104] J. Perez-Ramirez, C.H. Christensen, K. Egeblad, C.H. Christensen, J.C. Groen, Chem. Soc. Rev. 37 (11) (2008) 2530–2542.
[105] M. Kustova, K. Egeblad, C.H. Christensen, A.L. Kustov, Stud. Surf. Sci. Catal. 170A (2007) 267–275.
[106] R. Roque-Malherbe, V. Ivanov, J. Mol. Catal. A: Chem. 313 (1–2) (2009) 7–13.
[107] R. Harish, D. Karevski, G.M. Schuetz, J. Catal. 253 (1) (2008) 191–219.
[108] J. Kärger, R. Valiullin, S. Vasenkov, New J. Phys. 7 (2005) 15–30.
[109] (a) D.P. Serrano, J. Aguado, G. Morales, J.M. Rodriguez, A. Peral, M. Thommes, J.D. Epping, B.F. Chmelka, Chem. Mater. 21 (4) (2009) 641–654;

(b) D.P. Serrano, J. Aguado, A. Peral, Stud. Surf. Sci. Catal. 174A (2008) 123–128;
(c) D.P. Serrano, J. Aguado, J.M. Escola, J.M. Rodriguez, A. Peral, J. Mater. Chem. 18 (35) (2008) 4210–4218;
(d) D.P. Serrano, J. Aguado, J.M. Escola, J.M. Rodríguez, Á. Peral, Chem. Mater. 18 (10) (2006) 2462–2464.
[110] (a) S.J. Reitmeier, O.C. Gobin, A. Jentys, J.A. Lercher, J. Phys. Chem. C 113 (34) (2009) 15355–15363;
(b) S.J. Reitmeier, R.R. Mukti, A. Jentys, J.A. Lercher, J. Phys. Chem. C 112 (7) (2008) 2538–2544.
[111] (a) T.J. Pinnavaia, S.-S. Kim, Z. Zhang, Y. Liu, Stud. Surf. Sci. Catal. 154A (2004) 14–24;
(b) L. Frunz, R. Prins, G.D. Pirngruber, Micropor. Mesopor. Mater. 88 (1–3) (2006) 152–162.
[112] J.L. Zheng, S.R. Zhai, D. Wu, Y.H. Sun, Stud. Surf. Sci. Catal. 156 (2005) 119–124.
[113] G.-J. Kim, H.-S. Kim, Y.S. Ko, Y.K. Kwon, Macromol. Res. 13 (6) (2005) 499–505.
[114] K.S. Triantafyllidis, T.J. Pinnavaia, A. Iosifidis, P.J. Pomonis, J. Mater. Chem. 17 (34) (2007) 3630–3638.
[115] J. Zheng, D. Kong, W. Yang, Z. Xie, D. Wu, Y. Sun, J. Solid State Chem. 180 (2) (2007) 564–570.
[116] (a) S.-E. Park, K.-M. Choi, J. Phys. Chem. Solids 69 (5–6) (2008) 1501–1504;
(b) Y.K. Hwang, T. Jin, J.M. Kim, Y.-U. Kwon, S.-E. Park, J.-S. Chang, J. Nanosci. Nanotechnol. 6 (6) (2006) 1786–1791;
(c) Y.K. Hwang, J.-S. Chang, S.-E. Park, D.S. Kim, Y.-U. Kwon, S.H. Jhung, J.-S. Hwang, M.S. Park, Angew. Chem. Int. Ed. 44 (4) (2005) 556–560.
[117] (a) M. Choi, K. Na, J. Kim, Y. Sakamoto, O. Terasaki, R. Ryoo, Nature 461 (7261) (2009) 246–249;
(b) K. Na, M. Choi, W. Park, Y. Sakamoto, O. Terasaki, R. Ryoo, J. Am. Chem. Soc. 132 (12) (2010) 4169–4417.
[118] (a) A. Corma, V. Fornes, S.B. Pergher, Th.L. Maesen, J.G. Buglass, Nature 396 (1998) 353–356;
(b) A. Corma, V. Fornés, J. Martínez-Triguero, S.B. Pergher, J. Catal. 186 (1999) 57–63;
(c) A. Corma, V. Fornes, J.M. Guil, S. Pergher, T.L.M. Maesen, J.G. Buglass, Micropor. Mesopor. Mater. 38 (2) (2000) 301–309.
[119] (a) Y. Bouizi, I. Diaz, L. Rouleau, V.P. Valtchev, Adv. Funct. Mater. 15 (12) (2005) 1955–1960;
(b) Y. Bouizi, L. Rouleau, V. Valtchev, Chem. Mater. 18 (20) (2006) 4959–4966;
(c) Y. Bouizi, G. Majano, S. Mintova, V. Valtchev, J. Phys. Chem. C 111 (12) (2007) 4535–4542;
(d) V.P. Valtchev, Porous Materials with Hierarchical Organization, Key Note at International Zeolite Conference (IZC-IMMS 2010), Sorrento (Italy), July 2010.
[120] G. Yang, N. Tsubaki, J. Shamoto, Y. Yoneyama, Y. Zhang, J. Am. Chem. Soc. 132 (2010) 8129–8136.
[121] D. Chen, J. Wang, X. Ren, H. Teng, H. Gu, Catal. Lett. 136 (1–2) (2010) 65–70.
[122] J. Zheng, X. Zhang, Y. Wang, Y. Bai, W. Sun, R. Li, J. Porous Mater. 16 (6) (2009) 731–736.
[123] (a) V. Valtchev, Chem. Mater. 14 (3) (2002) 956–958;
(b) V. Valtchev, Chem. Mater. 14 (10) (2002) 4371–4437;
(c) V. Valtchev, J. Mater. Chem. 12 (6) (2002) 1914–1918.
[124] (a) W. Fan, M.A. Snyder, S. Kumar, P.-S. Lee, W.C. Yoo, A.V. McCormick, R.L. Penn, A. Stein, M. Tsapatsis, Nat. Mater. 7 (2008) 984–991;
(b) W.C. Yoo, S. Kumar, R.L. Penn, M. Tsapatsis, A. Stein, J. Am. Chem. Soc. 131 (34) (2009) 12377–12383.
[125] (a) A. Dong, Y. Wang, Y. Tang, N. Ren, Y. Zhang, Z. Gao, Chem. Mater. 14 (8) (2002) 3217–3219;
(b) A. Dong, N. Ren, W. Yang, Y. Wang, Y. Zhang, D. Wang, J. Hu, Z. Gao, Y. Tang, Adv. Funct. Mater. 13 (12) (2003) 943–994.
[126] Y. Zhang, Y. Liu, J. Kong, P. Yang, Y. Tang, B. Liu, Small 2 (10) (2006) 1170–1173.
[127] N. Ren, Y.-H. Yang, J. Shen, Y.-H. Zhang, H.-L. Xu, Z. Gao, Y. Tang, J. Catal. 251 (1) (2007) 182–188.
[128] M. Sastry, A. Swami, S. Mandal, P.R. Selvakannan, J. Mater. Chem. 15 (31) (2005) 3161–3174.
[129] (a) P.M. Arnal, M. Comotti, F. Schüth, Angew. Chem. Int. Ed. 45 (48) (2006) 8224–8227;
(b) P.M. Arnal, F. Schüth, F. Kleitz, Chem. Commun. (11) (2006) 1203–2120.
[130] S.D. Jackson, J.S.J. Hargreaves, Metal Oxide Catalysis, Wiley-VCH, Weinheim, Germany, 2009.
[131] G. Centi, F. Cavani, F. Trifirò, Selective Oxidation by Heterogeneous Catalysis, Springer, Heidelberg, Germany, 2000.
[132] G. Centi, F. Trifiro, J.R. Ebner, V.M. Franchetti, Chem. Rev. 88 (1) (1988) 55–80.
[133] (a) P. Chen, W. Xu, X. Zhou, D. Panda, A. Kalininskiy, Chem. Phys. Lett. 470 (4–6) (2009) 151–157;
(b) X. Zhou, W. Xu, G. Liu, D. Panda, P. Chen, J. Am. Chem. Soc. 132 (1) (2010) 138–146;
(c) H. Shen, W. Xu, P. Chen, Phys. Chem. Chem. Phys. 12 (25) (2010) 6555–6563;
(d) W. Xu, J.S. Kong, Y.-T.E. Yeh, P. Chen, Nat. Mater. 7 (2008) 992;
(e) W. Xu, H. Shen, G. Liu, P. Chen, Nano Res. 2 (12) (2009) 911–922.
[134] (a) R. Ameloot, M. Roeffaers, M. Baruah, G. De Cremer, B. Sels, D. De Vos, J. Hofkens, Photochem. Photobiol. Sci. 8 (4) (2009) 453–456;
(b) B.J.M. Roeffaers, B.F. Sels, H. Uji-i, F.C. De Schryver, P.A. Jacobs, D.E. De Vos, J. Hofkens, Nature 439 (2006) 572–575;
(c) G. De Cremer, M.B.J. Roeffaers, E. Bartholomeeusen, K. Lin, P. Dedecker, P.P. Pescarmona, P.A. Jacobs, D.E. De Vos, J. Hofkens, B.F. Sels, Angew. Chem. Int. Ed. 49 (2010) 908–911.
[135] M.A. Newton, Chem. Soc. Rev. 37 (12) (2008) 2644–2657.
[136] A.F. Lee, V. Prabhakaran, K. Wilson, Chem. Commun. 46 (22) (2010) 3827–4384.
[137] H.H. Rotermund, Surf. Sci. 603 (10–12) (2009) 1662–1670.
[138] T. Johannessen, J.H. Larsen, I. Chorkendorff, H. Livbjerg, H. Topsoe, Chem. Eng. J. 82 (1–3) (2001) 219–223.
[139] (a) G. Centi, S. Perathoner, in: J.J. Spivey, K.M. Dooley (Eds.), Catalysis, vol. 20, Royal Society of Chemistry, Cambridge, UK, 2007, pp. 367–394;
(b) G. Centi, S. Perathoner, in: J.J. Spivey, K.M. Dooley (Eds.), Catalysis, vol. 21, Royal Society of Chemistry, Cambridge, UK, 2009, pp. 82–130.
[140] G. Centi, R. Passalacqua, S. Perathoner, D.S. Su, G. Weinberg, R. Schlögl, Phys. Chem. Chem. Phys. 9 (2007) 4930–4938.
[141] (a) W. Ueda, M. Sadakane, H. Ogihara, Catal. Today 132 (1–4) (2008) 2–8;
(b) H. Ogihara, S. Masahiro, Y. Nodasaka, W. Ueda, J. Solid State Chem. 182 (6) (2009) 1587–1592;
(c) H. Ogihara, M. Sadakane, Y. Nodasaka, W. Ueda, Chem. Mater. 18 (21) (2006) 4981–4983.
[142] W.-N. Li, Vi.M.B. Crisostomo, E.K. Nyutu, Y.-S. Ding, S.L. Suib, in: W.V. Prescott, A.I. Schwartz (Eds.), Nanorods, Nanotubes and Nanomaterials Research Progress, Nova Science Pub., New York, 2008, pp. 203–238.
[143] F.s. Bozon-Verduraz, F. Fiévet, J.-Y. Piquemal, R. Brayner, K. El Kabouss, Y. Soumare, G. Viau, G. Shafeev, Braz. J. Phys. 39 (1A) (2009) 134–140.
[144] M. Willander, O. Nur, Q.X. Zhao, L.L. Yang, M. Lorenz, B.Q. Cao, J.Z. Perez, C. Czekalla, G. Zimmermann, M. Grundmann, Nanotechnology 20 (33) (2009), 332001/1–332001/40.
[145] N. Wang, Y. Cai, R.Q. Zhang, Mater. Sci. Eng. R: Rep. R60 (1–6) (2008) 1–51.
[146] T. Kasuga, M. Hiramatsu, A. Hoson, T. Sekino, K. Niihara, Langmuir 14 (12) (1998) 3160–3163.
[147] W. Wang, O.K. Varghese, M. Paulose, C.A. Grimes, Q. Wang, E.C. Dickey, J. Mater. Res. 19 (2) (2004) 417–422.
[148] C. Zhang, X. Jiang, B. Tian, X. Wang, X. Zhang, Z. Du, Colloids Surf. A: Physicochem. Eng. Aspects 257–258 (2005) 521–524.
[149] X. Feng, J. Zhai, L. Jiang, Angew. Chem. Int. Ed. 44 (2005) 5115–5511.
[150] T. Lai, L. Yi, W. Yang, Chem. Lett. 39 (3) (2010) 294–295.
[151] (a) T.A. Kandiel, R. Dillert, A. Feldhoff, D.W. Bahnemann, J. Phys. Chem. C 114 (11) (2010) 4909–4915;
(b) T.A. Kandiel, A. Feldhoff, L. Robben, R. Dillert, D.W. Bahnemann, Chem. Mater. 22 (6) (2010) 2050–2060.
[152] Z. Zheng, J. Teo, X. Chen, H. Liu, Y. Yuan, E.R. Waclawik, Z. Zhong, H. Zhu, Chem. Eur. J. 16 (4) (2010) 1202–1211.
[153] W. Smith, W. Ingram, Y. Zhao, Chem. Phys. Lett. 479 (4–6) (2009) 270–273.
[154] Z. He, Y. Li, Q. Zhang, H. Wang, Appl. Catal. B: Environ. 93 (3–4) (2010) 376–382.
[155] B. Liu, E.S. Aydil, J. Am. Chem. Soc. 131 (11) (2009) 3985–3990.
[156] (a) Y. Li, M. Zhang, M. Guo, X. Wang, Rare Metals 29 (3) (2010) 286–291;
(b) Y. Li, M. Guo, M. Zhang, X. Wang, Mater. Res. Bull. 44 (6) (2009) 1232–1237.
[157] X. Dong, J. Tao, Y. Li, H. Zhu, Appl. Surf. Sci. 256 (2010) 2532–2538.
[158] (a) C.A. Grimes, G.K. Mor, TiO_2 Nanotube Arrays Synthesis, Properties, and Applications, Springer, Heidelberg, Germany, 2009;
(b) S. Rani, S.C. Roy, M. Paulose, O.K. Varghese, G.K. Mor, S. Kim, S. Yoriya, T.J. La Tempa, C.A. Grimes, Phys. Chem. Chem. Phys. 12 (12) (2010) 2780–2800;
(c) K. Shankar, J.I. Basham, N.K. Allam, O. Varghese, G.K. Mor, X. Feng, M. Paulose, J.A. Seabold, K.-S. Choi, C.A. Grimes, J. Phys. Chem. C 113 (16) (2009) 6327–6359;
(d) C.A. Grimes, J. Mater. Chem. 17 (15) (2007) 1451–1457.
[159] (a) A. Ghicov, P. Schmuki, Chem. Commun. (20) (2009) 2791–2808;
(b) P. Roy, D. Kim, K. Lee, E. Spiecker, P. Schmuki, Nanoscale 2 (2010) 45–59.
[160] C. Ampelli, G. Centi, R. Passalacqua, R. Perathoner, Energy Environ. Sci. 3 (3) (2010) 292–301.
[161] M. Paulose, L. Peng, K.C. Popat, O.K. Varghese, T.J. LaTempa, N. Bao, T.A. Desai, C.A. Grimes, J. Membr. Sci. 319 (2008) 199–205.
[162] J. Wang, Z. Lin, Chem. Mater. 20 (2008) 1257–1261.
[163] S.P. Albu, A. Ghicov, J.M. Macak, R. Hahn, P. Schmuki, Nano Lett. 7 (2007) 1286–1289.
[164] (a) M.J. Climent, A. Corma, S. Iborra, ChemSusChem 2 (6) (2009) 500–506;
(b) A. Corma, Catal. Rev.: Sci. Eng. 46 (3–4) (2004) 369–417.
[165] A.J. Burke, V.R. Marinho, O.M.R. Furtado, Curr. Org. Synth. 7 (2) (2010) 94–119.
[166] P.N.R. Vennestroem, C.H. Christensen, S. Pedersen, J.-D. Grunwaldt, J.M. Woodley, ChemCatChem 2 (3) (2010) 249–258.
[167] J.M. Thomas, ChemCatChem 2 (2) (2010) 127–132.
[168] B.H. Shanks, Ind. Eng. Chem. Res. (2010), doi:10.1021/ie100487r.
[169] D.G. Vlachos, S. Caratzoulas, Chem. Eng. Sci. 65 (1) (2010) 18–22.
[170] Y. Traa, Chem. Commun. 46 (13) (2010) 2175–2187.
[171] G. Centi, S. Perathoner, ChemSusChem 3 (2) (2010) 195–208.
[172] R. Schlögl, ChemSusChem 3 (2) (2010) 209–222.
[173] J.-D. Grunwaldt, B. Kimmerle, A. Baiker, P. Boye, C.G. Schroer, P. Glatzel, C.N. Borca, F. Beckmann, Catal. Today 145 (3–4) (2009) 267–278.
[174] A.M. Molenbroek, S. Helveg, H. Topsoe, B.S. Clausen, Top. Catal. 52 (10) (2009) 1303–1311.
[175] G.A. Somorjai, J.Y. Park, Surf. Sci. 603 (10–12) (2009) 1293–1300.
[176] P. Sautet, F. Delbecq, Chem. Rev. 110 (3) (2010) 1788–2180.
[177] M. Neurock, in: U.S. Ozkan (Ed.), Design of Heterogeneous Catalysts: New Approaches based on Synthesis, Characterization and Modeling, Wiley-VCH, Weinheim, Germany, 2009, pp. 231–257.
[178] R.A. van Santen, P. Sautet, Computational Methods in Catalysis and Materials Science, Wiley-VCH, Weinheim, Germany, 2009.

[179] Q. Yang, D. Han, H. Yang, C. Li, Chem.: Asian J. 3 (8–9) (2008) 1214–1229.
[180] T. Ren, M.K. Patel, K. Blok, Energy 33 (5) (2008) 817–833.
[181] (a) G. Iaquaniello, F. Giacobbe, B. Morico, S. Cosenza, A. Farace, Int. J. Hydrogen Energy 33 (22) (2008) 6595–6601;
(b) S. Abate, C. Genovese, S. Perathoner, G. Centi, Int. J. Hydrogen Energy 35 (11) (2010) 5400–5409.
[182] S. Vajda, M.J. Pellin, J.P. Greeley, C.L. Marshall, L.A. Curtiss, G.A. Ballentine, J.W. Elam, S. Catillon-Mucherie, P.C. Redfern, F. Mehmood, P. Zapol, Nat. Mater. 8 (2009) 213–216.